ADDIS ABABA UNIVERSITY

ADDIS ABABA INSTITUTE OF TECHNOLOGY

DEPARTMENT OF CHEMICAL AND BIO ENGINEERING

Stastical process optimization on adsorption of phenol from water using Activated Carbon prepared from False banana (EnseteVentricosum) leaf

Prepared by: Mohammed Keder

A Thesis submitted to Addis Ababa Institute of Technology, School of Chemical and Bio-Engineering in partial fulfillment of the Requirement for the Degree of Master of Science in Chemical Engineering (Process Engineering)

Addis Ababa, Ethiopia

September, 2023

Addis Ababa University

Addis Ababa Institute of Technology

Department of Chemical and Bio Engineering

Process Engineering Stream

This is to certify that the thesis entitled "**Stastical process optimization on adsorption of phenol from water using Activated Carbon prepared from False banana (EnseteVentricosum) leaf**" and submitted in partial fulfillment of the requirements for the degree of Masters of Science (Chemical and Bio Engineering, Process stream) that complies with the regulations of the university and meets with the standard quality.

Approved by the Examining Board

Dr.AntenehWodaje		
Advisor	Signature	Date
Dr.ShimelisKebede		
InternalExaminer	Signature	Date
Dr.AntenehMarelegn	_____	_____
External Examiner	Signature	Date

DECLARATION

I declare that this thesis entitled "**Stastical process optimization on adsorption of phenol from water using Activated Carbon prepared from False banana (EnseteVentricosum) leaf**" has not been submitted in any form for another degree, diploma or an award at any university or institution of the tertiary education. I confirm that appropriate credit has been given within this thesis where reference has been made to the work of others and has been duly acknowledged. The work was under the guidance of Dr. Anteneh Wedaje instructor in Addis Ababa University, School of Chemical and Bio Engineering.

Name: Mohamed Keder

Signature:_____

Date:_____

ABSTRACT

The reason for this current study was to examine the potential of an adsorbent produced from EL to recover phenol from wastewater. Using agricultural wastes as valuable resources to create ACs from biomass wastes is one of the greenest resolutions. The main objective of this study was to use a chemical activation technique to produce ACs from readily available waste EL. An essential property for the synthesis of AC is the EL's cellulose concentration (18.4%), lignin level (10.3%), MC of 8.35%, VM of 71.09%, AC of 3.28%, FCC of 17.28%, and yield of 49.30% at 400°C. With a nitrogen flow rate of 150ml/min, the process of carbonization was conducted for 30, 60, and 90minutes at 400, 500, and 600°C. The char product was treated with 37% phosphoric acid (H_3PO_4) at diverse impregnation ratios (0.5, 1 and 1.5). It was found that 500°C, a 60-minute contact period, and an impregnation ratio of 1 in AC5 were ideal for the production of AC. With respect to surface area (1023m^2/g), iodine number (984mg/g), and total pore volume (0.45cm^3/g), AC5 was the largest. Scanning electron microscopy (SEM) analysis showed that the samples' uneven surface structure. Several functional groups that aid in adsorption was found when Fourier Transform Infrared Spectroscopy (FTIR) was examined. Using phenol as a separate adsorbate and the ideal conditions (PH=6, adsorbent dosage=0.4g, initial concentration=10mg/l, and contact time=120min) at room temperature, the adsorption capacity of generated activated carbon (AC5) was investigated. It was demonstrated that as initial concentration increased, the capacity of adsorption increased. The maximal phenol elimination capability of the AC_5 adsorbent is 95%. With the aid of the model, a relationship between the three experimental variables and the percentage of elimination was constructed. It looked into the phenol adsorption equilibrium isotherms utilizing the Freundlich, Temkin, and Langmuir isotherm models. For the concentration range of 10-150 mg/L, the monolayer adsorption capacity was 5.80mg/g, according to equilibrium data that followed the Langmuir model. There were kinetic analyses done. It was discovered that the data fit a pseudo-second order model. The best phenol elimination was obtained with an initial phenol PH of 6 and contact duration of 80 minutes. The study concluded that phenol could be effectively removed from aqueous solutions using activated carbon obtained from discarded Enset leaves.

***Key words**: activated carbon, Enset leaf, phenol, surface area, adsorption, and chemical activation.*

Acknowledgement

My first thanks are due to the Most Gracious and Merciful Allah, who has given me the courage and fortitude to continue working on my thesis. My sincere appreciation presented to my adviser, Dr. Anteneh Wedaje, for insightful criticism, counsel, as well as for his direction. Most importantly, though, I appreciate your prompt, accurate, and tireless revisions, which have really aided me in my research project. I am deeply indebted to Dr. Anurada for her excellent counsel and recommendations, which greatly enhanced the efficacy of my research endeavorsIn particular, I would like to convey my thankfulness to Mr. Asseged, Mr. Getu, and Mr. Walelign, the lab technicians at Addis Ababa Science Technology University's School of Chemical Engineering, as well as the lab technicians at Horizon Addis, for their positive cooperation and nonstop work during my laboratory work and characterization. Lastly, I would wish for to show gratitude my relatives for their amazing spiritual and financial support, inspiration, and advice during all of my great attempts. In particular, I would want to bestow this thesis to my father, Kedir Usman, who passed away very recently. May Allah be merciful to him, forgive all his sins, and let him enter Paradise.

Table of Content

Contents **Page number**

List of table

List of Figures

List of Acronyms

AC	Activated carbon
EL	Enset leaf
IR	Impregnation ratio
^oC	Degree Celsius
g	Gram
hr	Hour
t	Time
min	Minute
mm	Millimeter
cm^3	Centimeter cube
nm	Nano-meter
mg	Milligram
mgg -1	Milligram per gram
mgL-1	Milligram per litter
C_o	Initial concentration of phenol
C_e	Equilibrium concentration of phenol
q_e	Equilibrium adsorbed Amount of phenol
PH	Negative logarithm of concentration of hydrogen ion
K_1	Pseudo-first order rate constant
K_2	Pseudo-second order rate constant
K_L	Langmuir isotherm constant
K_F	Freundlich isotherm constant
R_L	Dimensionless separation factor
R^2	Correlation coefficient
H_3PO_4	Phosphoric acid
H_2SO_4	Sulfuric acid
NaOH	Sodium hydroxide
HCL	Hydrochloric acid

KOH	Potassium hydroxide
$ZnCl_2$	Zinc chloride
CO_2	Carbon dioxide
N_2	Nitrogen gas
CHNS	Carbon, Hydrogen, Nitrogen and Sulfur
BET	Brunauer-Emmett-Teller
BBD	Box-Behnken Design ANOVA Analysis of variance
FTIR	Fourier Transfer Infrared
SEM	Scanning electron microscope
TGA	Thermo Gravimeter Analysis
RSM	Response surface methodology

1. INTRODUCTION

1.1 Background

In the modern era, emissions have become a global issue of rising environmental concern because contaminants are continuously released into the environment, leaving behind residues in the air, water, and land. Because of industrialization, agricultural growth, and urbanization, there has been a rise in the usage of several hazardous chemicals as well as an increase in the use of water. Organic and inorganic contaminants, phenol and its derivatives also contribute to the pollution of water. Given their high toxicity and limited biodegradability, phenols and their derivatives are categorized as priority pollutants. This rapid expansion has caused widespread soil contamination, vegetable contamination, and most significantly, increased water body fouling(Minocha,2017).When treating wastewater, phenol has been removed using a variety of m ethods.Physical, chemical and biological elimination methods make up the three broad categories intowhich these methods are generally subdivided. Historically, phenol and related organic chemicals have been removed most frequently by solvent extraction, reverse osmosis, adsorption, catalytic oxidation, ion exchange, and biological treatment. In spite of this, the adsorption approach remains the most practical, quick, efficient, and economical way to get rid of phenol. A popular adsorbent for phenol removal is composed of easily obtained materials, such as leftovers from agriculture. These components consist of zeolite, chitin, clay, polymeric substances, red mud, and activated carbon. Commercial activated carbon has a particularly high affinity for phenol among these substances. Given the exorbitant price of commercial air conditioners and the associated regeneration process, this adsorbent is the least economical choice (Deng et al., 2017).

Treatment options for organic waste include stripping and oxidation, granular AC processes, electro Fenton method anaerobic processes, reverse osmosis, and other technologies (Busca et al., 2018). All of these are used to manage garbage, both biological and inanimate. The majority of the techniques have certain disadvantages, including high initial and ongoing expenditures, expenses associated with renewal, as well as waste disposal issues. Because of its ease of use, affordability of adsorbent, effectiveness, and availability of a wide range of adsorbents, liquid phase adsorption has proven to be a very successful and well-established technique for eliminating of organic compounds (Bandosz and selame, 2013). Because of its excellent

adsorption capacity, AC is frequently utilized as an adsorbent for eliminating of biological molecules.

The adsorption process that uses AC has several advantages: it is environmentally friendly, has a high effectiveness in eliminating pollutants even at extremely low concentrations, and is resistant to fouling by dangerous contaminants. The technique has been effectively employed as a solitary treatment process, mostly because of its capacity to eliminate a wide range of pollutants, increased adaptability, and accessibility to various adsorbent materials. Owing to these unique properties, AC is a very versatile material that has been investigated for use as catalysts and supports for a range of applications, such as the removal of impurities from gaseous or liquid phases and the purification or recovery of compounds, in addition to being used as an adsorbent.

The growing significance of carbon-based materials in managing pollution is driving the demand for activated carbon. Due to all of its applications, there is an increasing gap between the supply and demand for AC. Because of the exhaustible and unreasonable use of non-renewable and relatively expensive raw resources, such as pitch derived from coal or petroleum, were used in the attempt to prevent pollution. Furthermore, there is variability in their worldwide distribution. This trend may eventually lead to a shortage of supplies. Depending on surface performance, the intended use, carbon purity, thermal stability, chemical composition, and adsorptive capacity, it is imperative to investigate novel sources of based on carbon with the required physical and chemical characteristics, such as a high specific surface area. An increasing effort has been made to assess the feasibility and practicality of natural and recyclable materials as alternative adsorbents due to their complexity. In poor nations like Ethiopia, plants are thrown into the atmosphere after agricultural output is harvested rather from being used scientifically. This overview paper aims to discuss the details of the synthesis of AC from agricultural wastes as a potential adsorbent of harmful pollutants from waste water. The overview emphasizes on the benefits of using AC for agricultural waste adsorption over alternative waste treatment technologies. This might indicate a potential topic of focus for academic research aimed at improving technologies.

1.2 Problem statement

Most prevalent agricultural waste categories worldwide, producing millions of tons annually, most of which are either burned or dumped in landfills. In addition to seed pods and shells, crop wastes include the leaves of many fruit plants, corn husks, and the straws of rice, oats, barley, and wheat. It is anticipated that more than 2802 million metric tons of this garbage will be produced annually worldwide. With almost 750 million tons produced per per year, corn stalks are the most abundant crop waste, followed by rice and wheat with 600 and 360 million metric tons produced annually, respectively. Because of their high carbon content, these organic wastes make a desirable starting material for preparation of AC. The byproducts from corn, wheat, and rice crops are mostly thrown into landfills or burnt outdoors, with just a tiny percentage being effectively used in certain uses like animal feed and/or the creation of bio-energy. On a chemical level, crop leftovers include microelements and phosphorus required for crop growth, along with 40–45% carbon, 0.6–1% nitrogen, and 14–23% potassium.

Using materials such nutshells, coconut shells, apricot stones, and plum stones has been the subject of a ton of literature (Nadavala et al., 2020). In contrast, there has been significantly less focus on the manufacture of AC from enset leaf. Meeting this need is made possible by the wide range of activation techniques described, the amount of raw materials available for the production of AC, and the variety of AC available on the market. Therefore, ongoing research is necessary to provide quality AC for certain applications.

1.3 Objectives of the study

The purpose of this study is to assess the stastical process optimization on adsorption of phenol from water using EL AC. In order to accomplish them, a study was conducted with the following precise goals:

i. To investigate the potential of prepared activated carbon.
ii. To investigate the characteristics of the prepared activated carbon.
iii. To investigate impact of carbonization temperature, holding time and chemical activation on the creation of pore structure and yield.
iv. To determine the adsorption capacity of AC using optimum initial concentration of phenol, contact time, PH, and adsorbent dose.
v. To optimize the adsorption control parameters to get optimum removal efficiency.

1.4. Significance of the study

The study presents AC, which is produced locally using resources that are high in carbon and low in inorganic matter. Thus, this study offers useful information for future research about the availability of EL waste for the production of AC and the effectiveness of phenol removal from water streams.

1.5 Scope of the study

The current study used the chemical activation method to make EL AC by varying process parameters, including carbonization temperature, holding time, and impregnation ratio. The activated carbon was then characterized by FTIR, TGA, BET surface analysis, ultimate analysis, and proximate analysis. Lastly, phenol was extracted from water using an adsorption test.

2. LITERATURE REVIEW

2.1 Phenol

Because phenols have hydroxyl groups in their structures, they are similar to alcohols in several ways. They are able to create powerful hydrogen bonds. In addition, these substances have greater boiling points than the same molecular weight hydrocarbons. Since phenols can create strong hydrogen bonds with water molecules, they are additionally modestly soluble in water. Alcohols are weaker acids over phenols. Phenoxide ions are produced when they combine with bases such as sodium hydroxide. Nonetheless, they do not react with sodium hydrogen carbonate and are weaker acids than carboxylic acids. In the majority of their reactions, phenols exhibit nucleophilic behavior, while the reagents that interact with them exhibit electrophilic behavior. The hydroxyl group or aromatic ring of phenolic compounds can be the location of nucleophilic reactivity. Electrophilic aromatic replacement is the outcome of the reactions that are conducted on the aromatic ring.

(a) Halogenation: Even in the absence of a catalyst, phenols can be readily brominated and chlorinated. The para position is where substitution to the hydroxyl group generally takes place. Ortho-substitution is used when the para position is blocked.

(b) Nitration: In either water or acetic acid, phenol reacts with diluted nitric acid. Because phenolic chemicals are highly reactive, nitric and sulfuric acid combinations are not required.

(c) O-nitrophenol is an ortho-substituted phenolic molecule, its boiling point is significantly lower than that of its meta and para isomers. This is because the energy needed to transition from the liquid to the vapor phase is partially offset by the hydrogen bond that forms between the hydroxyl group and the substituent.

(d) Nitrosation: In the acidification of sodium nitrite, a weak electrophile, combines with a phenol's strongly activated ring to produce the nitrosonium ion [N ≡ O+]. One byproduct of the process is nitrosophenol.

(e) Sulfonation: Concentrated sulfuric acid and phenol can react to cause the ring to sulfonate.

(f)Friedel-Crafts alkylation: Carbocations are produced when acids and alcohols are combined. The alkylation is caused by a carbocation attacking a phenol's electron ring.

Phenolic compounds can be found in multiple uses such as adhesives, foams, emulsifiers, detergents, pesticides, dyes, explosives, flavors, and rubber chemicals. They can also self-assemble into nanomaterials, resins, and other materials (Kabinge I, 2018).

2.1.1 Phenol removal technologies

Conventional techniques like extraction, distillation, chemical oxidation, electrochemical oxidation, and adsorption can effectively remove a large number of phenolic chemicals. Therefore, before being released, trash contaminated with phenolic chemicals at both low and high quantities needs to be treated. Here are some current techniques that are explained:

(a) Membrane processes: To eliminate organic pollutants, membrane processes are used in the treatment of water and wastewater. This method is currently being researched for the removal of phenolic chemicals. Their key benefits include low energy usage, low operating costs, and simple scalability via membrane modules. With a burgeoning potential for industrial applications in biotechnology, nanotechnology, and purification processes, separating membranes offer a multitude of uses in modern times.

(b)Nanofiltration and reverse osmosis: Reverse osmosis is a membrane-based demineralization process used primarily to extract ions and other dissolved solids from aqueous solutions. However, the removal of organic contaminants, inorganic salts, color, and hardness from aqueous solutions is a common use of nanofiltration. It helps lower the pressures related to organic materials when used before a reversible osmosis unit.

(c) Chemical oxidation: Phenolic compounds can be destroyed by chemical oxidants. The procedures operate under mild conditions (temperature and PH), consuming little energy and reagents. The most often used chemicals in the oxidative procedure for polluted water include ozone, chlorine, chlorine dioxide, chloramines, ferrate [Fe (VI)], and permanganate [Mn (VII)].

(d) Electrochemical oxidation: This method works well for oxidizing a wide range of organic pollutants at high chloride concentrations, which are typically greater than 3g/L. Any further phenol-destroying method that doesn't require the addition of chemicals is electrochemical oxidation. There are two types associated with this technique: indirect and direct oxidation. Adsorption of impurities onto the anode surface results in direct, or anodic, treatment. A variety of anode materials are employed, the most studied ones being Pt, PbO_2, SnO2, IrO_2, and BDD (boron-doped diamond). Process efficiency is greatly impacted by factors like current density, PH, anode material, and electrolyte usage.

(e) Advanced oxidation processes: These methods have one thing in common: they produce hydroxyl radicals spontaneously, which are free radicals that can mineralize most organic materials, including molecules that include phenol. They are primarily employed in the remediation of contaminated waterways containing organic materials that are resistant to treatment, such as pesticides, surfactants, coloring agents, and medications.

(f) Biological treatment: For aqueous phenols, biological treatment is the method most frequently used. The process is a low-cost, easily maintained way of turning phenolic solutions into straightforward final products.

(g) Technology of adsorption: A surface phenomena known as adsorption occurs when one or more fluid (gas or liquid) components are attracted to the surface of a solid and physically or chemically bond. It is possible for adsorptions to be chemical or physical. Physical adsorption occurs when reversible intermolecular Vander Waals forces attach the adsorbing molecule to the solid; this process is known as Vander Waals adsorption (Patel, 2021). Chemical adsorption was also referred to as chemisorption. They defined this term as the irreversible covalent or ionic connection between the molecules that are being adsorbing and the solid. Adsorption works well in most biological, natural, chemical, and physical systems, and is widely used in commercial applications (Odoemelam and Charles, 2018). ACs Widely utilized in adsorption.

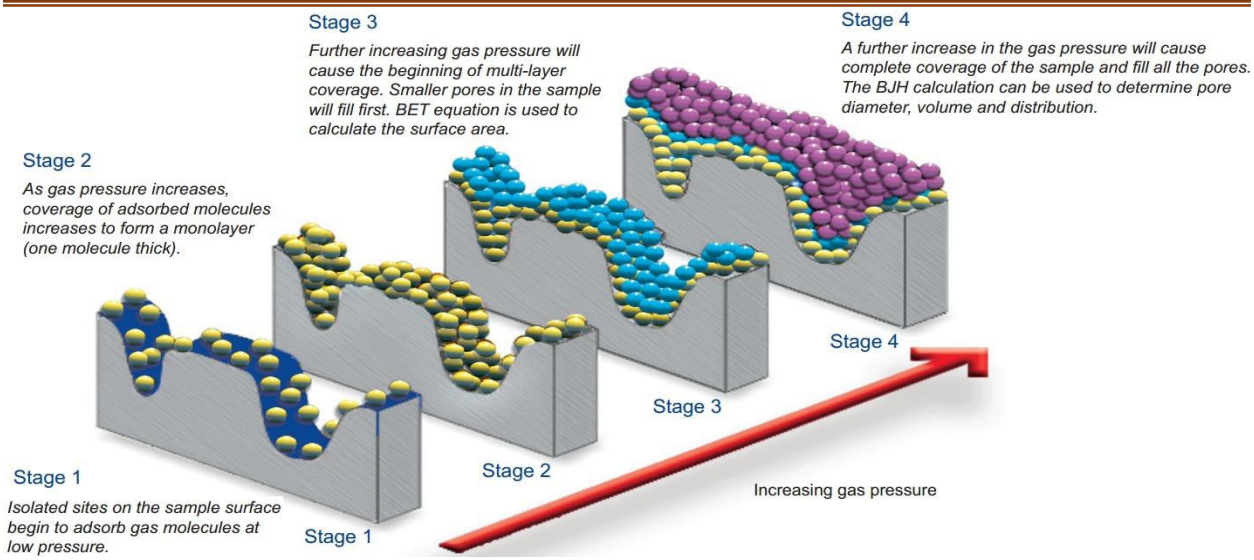

Fig. 2.1: The adsorption process's four phases (Lowell et al., 2012).

2.1.2 Factors affecting adsorption

According to (Soto et al., 2019), the following factors can alter adsorption:

(i) Pore size, surface functional groups and Surface area are examples for physical and chemical attribute of the adsorbent.

(ii) Properties of adsorbate such as the PKa of the multicomponent or binary solution.

(iii) Liquid phase adsorbate concentration.

(iv) Characteristics of liquid phase, such as pH and temperature.

(v) The process's length of stay.

(Vii). Adsorbent dose

2.2 Activated carbon (AC)

AC comprises a broad range of amorphous carbon-based materials that have been manufactured to exhibit a high degree of porosity and a prolonged interparticulate surface area. It also refers to a class of crystalline adsorbents that have notable internal pore patterns that increase the carbon's absorbency. It can alternatively be defined as a carbonaceous material with a highly developed

porous structure and a sizable internal surface area that is created when raw materials are processed at high temperatures. Its makeup varies between 87% and 97% carbon, but depending on the source material and processing method, it may also contain other elements. AC has the ability to absorb materials from both the liquid and gas phases because of its porous structure. Its pore capacity is typically found to be as large as $1cm^3$ per gram, but it can range from 0.20 to $0.60cm^3$ usually. Its surface area typically ranges from 800 to 1500 m^2/g, however studies have found values as high as $3{,}000m^2/g$. Lazo-Cannata et al. (2019) report that micropores with pore diameters less than 0.02 mm comprise most of the surface area. These benefits have made activated carbon a popular adsorbent for a range of benefits.

2.2.1 Types of activated carbon

AC firstly was made in the United States using black ash, which was used as the source after it was inadvertently found to be quite effective at discoloring liquids. It has been widely used for the removal of organic dyes in several industries, including the textile industry. The main applications for powdered ACs are flue gas treatment and adsorption in liquid phase. Powdered AC is most commonly used in wastewater treatment through a secondary treatment process called the powdered AC treatment process (Norit Americas Inc., 2020).

Because of its significantly larger particle size, granulated activated carbon has a lesser external surface area than powdered activated carbon. The sizes range from 0.5 mm to 4.0 mm. Water treatment facilities commonly use the granular carbon bed used in this type of activated carbon bed to eliminate tastes, colors, odors, and dissolved organics. In the gas phase, granular activated carbon can also be used.

There are three different forms of AC on the market right now: pellet, powder, and granular. It is divided into many types based on the shapes and sizes of its particles, and each form has a particular use. The average diameter of activated carbon powder is between 0.015 and 0.025mm, with a size smaller than 0.001mm. As a result, they display a huge interior surface and a close diffusion distance. The extruded and cylindrically shaped activated carbon used to make pellet activated carbon has diameters between 0.04 and 0.07mm and a length between 0.08 and 0.015mm. Due to their low pressure drop, excellent mechanical strength, and low dust content, pellets of activated carbon are mostly used in gas phase applications.

2.2.2 Characterization and Properties of Activated Carbon

To classify AC for certain uses, characterization is crucial. Essentially, AC is distinguished by its physical and chemical characteristics. According to Guo and Lua (2020), the physical and chemical characteristics of the raw materials as well as the activation method used determine the features of activated carbon. The physical properties of granular AC, including as their moisture and ash contents, might affect how they are used and whether or not they are suitable for a certain application. Although the specific surface area and surface chemistry of activated carbon are regarded as chemical properties. The porous structure of activated carbon can also be studied using a variety of methods, such as scanning electron microscopy and the adsorption of vapors (water, benzene) or gases (Ar, Kr, CO_2, N_2O).

(a) Moisture Content

AC is typically valued based on free of moisture, however on occasion specific moisture content 8 to 10%, is specified.

(b) Ash content

It is ruminant of burning up the carbonaceous components. When used activated carbon regenerates, the presence of ash can induce a restructuring process, increase hydrophilicity, and have catalytic effects. According to Yang (2017), the amount of inorganic material in activated carbon is determined by its ash concentration, which normally varies from 2 to 10%. To assess the amount of ash present, a weighed quantity of is heated in a muffle furnace until the carbon is completely burned. In order to maintain the inorganic components' volatilization and the ash's appropriateness for additional examination, the temperature should be kept below 600°C.

(c) Surface area

The most popular commercial active carbons have a S.A of between 600 and 1200m^2/g. The amount of material that can be adsorbed, given an appropriate molecular size, is limited by the surface area, whereas the pore volume limits the size of molecules that may be adsorbed. An adsorbent's internal surface area and pore volume determine how much of it can absorb. The adsorption capacity of an adsorbent is determined by its specific S.A. Typically, gas adsorption measurements are used to quantify the S.A using the Brunauer-Emmett-Teller (BET) theory (Srinivasan and Hu, 2018). Analyzing an adsorption isotherm is the most popular technique for

describing these structural traits of the porosity. Nitrogen is the principal adsorptive at 77K, though argon can be employed.

(d) Surface Functional Group of Activated Carbon

The ability to alter the surface chemistry of AC would be ideal for various applications in order to boost effectiveness. The surface chemistry is influenced by the chemical composition of the raw materials, which may offer a less expensive method of altering the properties of activated carbons. For example, it has been found that the conversion of SO2 to sulfuric acid may be catalyzed very well using activated carbon fiber that is formed from nitrogen-rich isotropic pitches (Radovic, 2017).

Numerous functional groups incorporating oxygen, nitrogen, and other hetero atoms have been found on AC. Heteroatoms are easily able to aggregate on the surface during the carbonization and activation processes employed in manufacture because of the large porosity and multiple disordered spaces present in activated carbons. Heteroatoms are integrated into the network in addition to being confined to the plane edges. In their reactions with different reagents, the heteroatoms adhered to the surfaces adopt the properties of the functional groups often seen in aromatic compounds. These surface groups are essential to the surface chemistry of activated carbon, claims Yang (2017).

Surface functional groups can be determined using a variety of techniques made to examine the functional groups using spectroscopic, such as infrared (IR) light.

(e) Pore size

One of the characteristics of activated carbon that has a big impact on how well it works and is used in adsorption is its pore size. The method of heat pretreatment facilitates the formation of pores in the biomass waste by removing moisture and volatile chemicals. These holes can then be utilized for entrapment, attachment, or beneficial application in the adsorption process. Agarry and Aremu (2019) claim that the pore structure of AC influenced by the biomass's content. Higher lignin percentage in biomass results in AC with a macro porous structure, whereas higher cellulose concentration results in mostly micro porous activated carbon. Although mesopores may serve as the transport medium to micro pores, attachment or trapping of solute molecules during the adsorption process primarily takes place in micro pores. Micro pores therefore play the biggest role in how well AC works. The elimination of moisture and

volatile materials from the biomass waste during heat pretreatment enables the creation of pores, and these pores then serve as locations for entrapment, attachment, or useful application during the adsorption process. The composition of the biomass affects the pore structure of activated carbon. While biomass with higher cellulose concentration produces activated carbon with primarily micro porous structure, those with higher lignin content produce it with a macro porous structure. Although mesopores may serve as the transport medium to micro pores, attachment or trapping of solute molecules during the adsorption process primarily takes place in micro pores. Micro pores therefore play the biggest role in how well activated carbon works.

2.2.3 Processing of activated carbon

AC is processed primarily by choosing factors that impact carbonization, the formation of activated carbon, and the types of activation.

(a) Carbonization

The precursors are pyrolyzed to produce carbon dioxide in an inert atmosphere. This will increase the organic materials' carbon content. The holes that are created during the carbonization process are typically small and occasionally blocked by tarry materials. Tar-like compounds begin to accumulate when components of the volatile carbon matrix permeate into the gas main stream from the pore structure. Certain substances may react with the pore walls, resulting in hydro cracking and carbon deposition, claims Kamishita (2018). This effect was seen when producing activated carbon from guava seeds. As a result, the carbonization byproducts constricted the pores, causing the organic contents to partially disintegrate, and the resulting activated carbon was poor at adsorbing (Rahman and Saad, 2020).

(b) Activation

Physical and chemical activation are the two main categories of activation, according to Varil et al. (2017).

(i) Physical activation

Van der Wall weak forces, hydrogen bonds, and interactions between the sorbent and sorbet's dipoles are all components of physical sorption. It can be undone and is similar to the condensation process. According to Cooney and David (2016), the physisorption process is exothermic and has an adsorption heat similar to the latent heat of condensation. Two steps make up the physical activation process. Char is created by the carbonization of carbonaceous

materials. The char is activated at a high temperature while being exposed to activating chemicals such CO_2, steam, air, or their combinations.

The raw precursors or char are oxidized using an oxidizing gas at 800-1100°C to execute physical activation, with the goal of achieving a specified percentage of burn-off. However, the temperature must be selected cautiously. Lower temperatures cause the reactions to happen too slowly. At lower temperatures, reactions start on the inside surface of carbon. Diffusion-controlled reactions occur on the outside of carbon atoms at higher temperatures.

As reported in the literature, physical activation of bio-based activated carbons resulted in poorer sorption capabilities for anionic pollutants than chemical activation (Xu et al., 2019).

(ii) Chemical activation

It uses chemical agent prior to activation. The chemical agents such as KOH, NaOH, $ZnCl_2$, H_3PO_4 and H_2SO_4, are commonly used. Activation procedure involves impregnating the material with the chosen chemical either solidly or liquidly. Such impregnation can take up to 24 hours, based on the sample, procedures and chemical used. Of paramount importance are the ratio of chemical to precursor, temperature, and retention time. A cleaning step is also necessary, either with mild acid or distilled water, to remove any leftover chemicals from the material (Paraskeva et al., 2018).

The processes of carbonization and activation occur simultaneously in the presence of activation chemical (Altintig & Kirkil, 2016). Since the inorganic components of the used agents might contaminate the environment and corrode equipment, additional washing procedures are necessary (Hong et al., 2016). The activating chemicals influence breakdowns pyrolytically by dehydrating including inhibit the formation of tar, according to Erdem et. al. (2016). A lot of work has gone into creating activated carbons with the right pore structure and surface properties through chemical activation.

According to Gottipati and Mishra (2019), the preparation process factors that influnce the development of pores in AC include type of chemical agent utilized for activation and the type of precursor that was used. Adjustments are made to carbonization temperature, impregnation time, and chemical agent ratio for best preparation. The raw material and the activation procedure have a high persuade on the features of product.

Chemical activation has the potential to dramatically alter the properties of bio-chars. For example, H_3PO_4 has been employed as an activation agent to convert biomass into AC. H_3PO_4 activation has enhanced porosity, generated a comparatively higher carbon yield, and created P-containing functional structures on treated AC. Phosphoric acid is commonly used as an activating agent when converting lignocellulose materials into ACs. This is because of its advantages, which include being less toxic than zinc chloride and being easily removed by leaching with water. After recovery, the phosphoric acid is recycled for more applications Activated carbons are usually manufactured from lignocellulose materials and activated by treating them with phosphoric acid in order to decolorize or remove organic impurities from liquids. Of all the activators in Table 4, it is clear that H_3PO_4 is the one that is used the most. This could be the result of acidic activation being less beneficial economically and required activation being more expensive. H_3PO_4 is a further economical method that gives a larger percentage of yields (Din et al., 2017). The mesopores and micro pores are also altered during this process, which significantly affects the final product's porosity, reactivity, and surface area. Arami-Niya et. al. (2021) investigated the effects on the oil palm shell textural properties of neutral and acidic activation using $ZnCl_2$ and H_3PO_4. It has been observed that surfaces and pore volumes generated by acidic activation are larger than those generated by neutral activation. It is reasonable, according to Arami-Niya et al. (2019), that the speed of activation which is higher for H_3PO_4 with an 8.86% burn-off per hour and $ZnCl_2$ with a 22% burn-off per hour is what causes the variations in qualities of texture.

H_3PO_4 is frequently employed to make AC from biomass. The generation of ACs by activating woody biomass using phosphoric acid at 600°C with in inert environment was studied by Budinov. It was discovered that the adsorptive ability of the AC rose with 30% when the H_3PO_4 concentration was raised from 20% to 50%.

A distinct carbonization and activation process was also used to prepare samples for the ensuing chemical activation. Precursors were created using a range of purging gases and heated to 500°C for 2hrs before being impregnated with 50% H_3PO_4. It was found that air purging gas was necessary to produce the maximum surface area AC. According to Tay et. al. (2019), there is less need for char burn off, which results in shorter treatment periods, higher yield, and the production of ACs with more porosity and surface area. Moreover, ACs created by chemical

activation has greater porosity than those created by physical activation. The disadvantages of chemical activation include the cost of the activating agent, the requirement for a second washing step to get rid of the chemical agent, the high solubility of oxygen, the high autogenic pressure at high temperatures, and the possibility of activating agents corroding in solution. According to Kong et. al. (2016) and Dias et. al. (2007), there is a need for a second round of neutralization and the cost of the activating agents is higher.

2.2.4 Factor affecting AC Production

(a)Raw material

The majority of carbon-rich organic materials that don't combine during carbonization can be used as raw materials to create AC (Rodriguez-Reinoso, 2020). Several criteria are taken into account while choosing the raw material to make porous carbon.

These elements are:

i. A high amount of carbon

ii. Has a low inorganic content, or little ash.

iii. Enough VC and high density

iv. Stable supply.

v. The possible level of activation

vii. Cheap materials

vii. Minimal deterioration after storing

Lignocellulosic material is the most widely utilized precursor, accounting for approximately 45% of all raw materials used in the production of AC. To produce AC low organic material content with minimal ash, is essential, but relatively high volatile content is also needed to manage the production process. Further details about the characteristics of the raw ingredients that go into making AC can be found in Table 2.1.

Table2.1 raw materials used for preparation of AC and their characteristics
(Manocha, 2003)

Raw materials	Volatile (%)	Ash (%)	Carbon (%)	Texture of AC

Soft wood	55-60	0.3-1.1	40-45	Soft, large pore volume
Hard wood	55-60	0.3-1.2	40-42	Soft, large pore volume
Lignin	58-60	-	35-40	Soft , large volume
Nut shells	55-60	0.5-0.6	40-45	Hard, large multi volume
Lignite	25-40	5-6	55-70	Hard, small pore volume
Soft coal	25-30	2.12	65-80	Medium hard, medium micro pore
Petroleum coke	15-20	0.5-0.7	70-85	Medium hard micro pore volume
Semi hard coal	1-15	5-15	70-75	Hard, large pore volume
Hard coal	5-10	2.15	85-95	Hard large volume

Recent research has examined agricultural leftovers and byproducts as possible preliminary resources for synthesis of ACs, given their high disposal costs, low economic value, and abundance of renewable resources.

You may also utilize peach stones to create premium activated carbons. According to measurements, the ACs formed using peach stones treated with H_3PO_4 at 500°C had a pore volume of 0.83cc/g and a surface area of 1400 m^2/g (Parker, I., 2018). The yield of the finished product ranged from 40% to 43.8% depending on the percentage of phosphoric acid. AC made from peach stones was found to have less porosity and a lower capacity to adsorb methane blue after being thermally treated by pyrolyzing the carbon in N_2 for an hour at 800°C.

AC was produced by a single-stage chemical activation process with rice husks, with a retention period of 30 to 60 minutes. The greatest surface area of the activated carbon obtained from impregnating rice husks with $ZnCl_2$ at a ratio of 1:1 at 700°C was 750 m^2/g, but the activated carbon prepared from bagasee at a ratio of 0.75:1 at the same temperature was 674 m^2/g. Compared to activated carbon derived from other biomass sources mentioned in the literature, AC derived from rice husks has a slightly smaller surface area. This could be because the high

16.1% ash content of the rice husk prevented the activated carbon's porosity from growing. Furthermore, it was found that when temperature and retention time increased, the ACs' surface area reduced since this led to an increase in tar formation, which impeded the development of porosity.

(b) Temperature

The distinctiveness of the created AC are influenced by temperature, especially the final activation temperature. According to numerous authors, carbonization temperature has a big impact the surface area of AC as well as on the output of AC synthesis. 200°C and 1100°C (San Miguel, et al., 2019) lowest and highest temperature was employed.

Regardless of impregnation ratio and activation time for different raw materials, the majority of earlier studies claimed that the optimal temperatures ranged from 400 to 500 °C (Srinivasakannan and Zailani, 2019). As the temperature of activation rises, the yield of activated carbon consistently declines. It was hypothesised that as the temperature of carbonization rose, the amount of volatile matter decreased, with the greatest variation in this parameter happening between 200°C and 800°C due to the region's fast carbonization. Furthermore, as there is very little decline in volatile matter above 800 °C, it is not acceptable to set up AC at carbonization temperatures higher than this range. It accompanies by an increase in the amount of ash and fixed carbon, which is explained by the material's volatile components being removed during the carbonization process leaving behind the more minerals that produce carbon and ash. Another interesting feature that shows how the activation temperature influences the properties of activated carbon is the BET surface area. As the activation temperature increased, so did the BET surface area (Emeish and Haimour, 2019). It could explain by expanding existing holes when the carbonization temperature rises and the formation of innovative pores due to volatile mater being released.

(c) Holding time

The properties of AC and carbonization process are also imposed by the activation duration in addition to activation temperature. According to earlier research, the typical activation durations for palm and coconut shells were between one and three hours (Srinivasakannan and Zailani, 2019). The yield percentage significantly reduced over time, and the BET surface area likewise grew. The formation of AC due to organic components volatilization in the raw material may be

the cause of this outcome. When excessive activation takes place, it is seen that the degree of the decline in product yield is lowering (Kim et. al., 2021).

2.2.5 Applications of AC

In numerous industries, including adsorption, aqueous-phase treatment, and super capacitors, activated carbons are useful.

Fig. 2.2: Applications of activated carbon

2.3 Enset

Enset, scientifically, known as Enseteventricosum. In terms of morphology, banana plant is similar to Enset. Its features underground stem structure called corm, a pseudo stem, huge leaves, and root system. However, it is grown-up primarily for its underground corm and pseudostem base, which are used to make starchy food items, rather than for its fruits. Especially in Ethiopia's south and southwest highlands is Enset cultivated, and for over 24 million people (about 20% of the country's people), it is a staple diet. The enset tree is another native plant that grows wild in many countries, including sub-Saharan Africa. It is the main crop of an endemic African system that is drought-tolerant and perennial. Over 200,000 hectares of the highlands in Ethiopia's southern, southwest, and central are home to the drought-resistant plant Enset. Harvesting typically took place in six up to seven years after the flower appears on the Enset plantings. But if there is a lack of food or cattle feed, the harvesting may took place at any time (Blomme et. al. Citation2023).

Fig. 2.3 Enset plant

2.4 Gaps on Activated carbon

Newly constructed factories in Ethiopia employ AC as one of their fluid waste management means. Ethiopia has the capacity to create AC, however these recently developed companies spend a significant amount of money importing it (Elyas K, 2017). Because of this, production of AC from agricultural waste can be considered as a means of reducing the currency expenditure for AC. There is a ton of literature on the usage of lignocellulosic materials like nutshells, coffee husk, saw dust and plum stones. The preparation of AC using enset leaf, on the other hand, got far less attention. From the potential raw materials which can found locally is EL is one of them. Therefore, this study emphasize on assess the potential EL for preparation of AC for removal of phenol from water.

3. MATERIALS AND METHODS

3.1 Chemicals

Analytical grade reagents and chemicals were used in this investigation. From these, the necessary chemicals that used in this study were; distilled water, phenol (purity level of >98%), phosphoric acid (37% by mass), hydrochloric acid and sodium hydroxide (0.1 M solutions) and, standardized iodine, Sodium thiosulphate pent hydrate and starch.

3.2 Apparatus and Instruments

Beakers, Erlenmeyer flasks, funnels, graduated cylinders, pipettes, spatulas, suction filtration flasks, measuring cylinders, conical flasks, filter paper, magnetic stirrers, electric motors, sieves, electronic balances, electric ovens, centrifuges, filter paper, Furnace elemental, surface area analyzers, UV visible Spectrophotometers (JASCO UV/Vis-550), FTIR (FTIR RX-1, PerkinElmer, USA) spectrometers, and 5500 EUTECH PH Meters were among the equipment and instruments used in this study.

3.3. Experimental Methodology

3.3.1 Enset leaf Preparation

For this study, from a neighboring Enset cultivated field EL wastes around 6 kg were gathered. After a thorough cleaning to remove any remaining dust and debris, they are finely cut into tiny pieces. The cleaned EL was left out in the open to allow moisture to escape from its surface before being dried for 12hours at 105°C to eliminate extra moisture. The EL were completely dried before being broken up and ground into powder. The EL are ground, separated into different-sized particles, and then maintained in airtight containers for activation (Rashidi&Borhan, 2014).

Fig. 3.1: Raw, sun dried and Powdered Enset leave

3.3.2 Activation of carbonized Enset leaf

For the purposes of this experiment, Enset plant debris weighing around 6kg was collected from a neighboring Enset cultivated area. The carbonizing temperature, impregnation ratio, and length of carbon activation are the variables that are changed throughout the activation phase of activated carbon made from EL. In this investigation, the activating agent used was phosphoric acid (37% H_3PO_4). Phosphoric acid was chosen for this study based on earlier research on similar lignocelluloic precursors. Comparing results with current chemicals, the aforementioned chemical exhibits superior pore formation in activated carbon (Borhan & Kamil, 2012). The impregnation ratios that were examined in this experiment were 1:0.5, 1:1, and 1:1.5. The weight of the dried powder EL (W_{EL}) divided with the dried activating ingredient weight (W_{H3PO4}) yields the impregnation ratio.

Impregnation ratio = W_{EL} / W_{H3PO4} (3.1)

After being combined with powdered Enset dust impregnated with nitrogen gas (N_2), the remaining material is then carbonized in a tube furnace under a continuous stream of N_2. The temperature required to rise by about 10°C every minute. In order to prevent the samples from oxidizing and moving volatile materials out of the heating zone the atmosphere became inert using N_2 gas. Temperature of 400, 500, and 600°C were determined for carbonization process and were held for 30, 60, and 90 minutes, respectively. The precursors were first burned, after that impregnated in a furnace, and then they were quickly moved to desiccators (moisture sacks) to prevent oxygen contact before being allowed to cool to room temperature (Borhan, 2014).

10g of carbonized EL were combined with a volume of 100mL H_3PO_4, and the mixture was left to soak overnight. This method used to make sure that the chemicals are fully drenched and adsorbed into the powdered EL. Covering of the container with foil helps to keep the mixture of powdered EL and phosphoric acid (37% H3PO4) from getting contaminated or from evaporating.

Fig.3.2: Carbonized EL powder soaked in H_3PO_4

Subsequently, the chemical agents are extracted from the leaf impregnated with Enset (Rashidi 2014). Following carbonization and activation, the resulting activated carbons underwent a thorough washing in hot distilled water until their pH achieved neutrality.

Fig. 3.3: Filtration of soaked Enset leave using hot distilled water

After being grounded and sealed in plastic bags for later usage, activated carbons were finally dried for 24hours at 105°C in an oven. Enset leave powder particle sizes, which are 0.25mm, are employed for each set of parameters. For all the parameter combinations under examination, a total of 27 samples must be created.

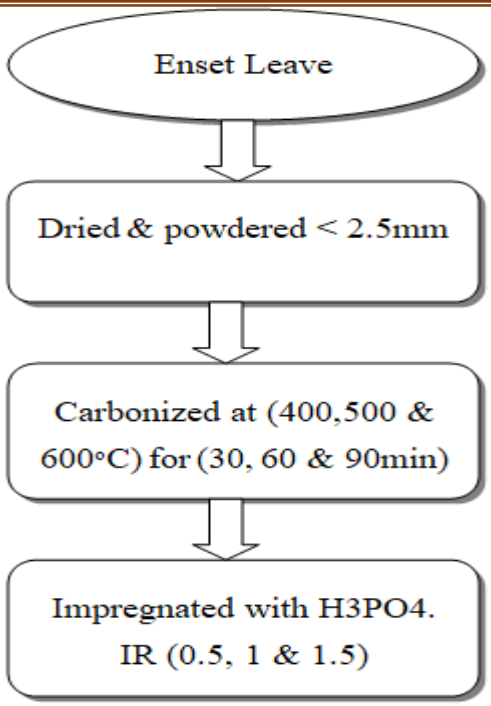

Fig. 3.4: Procedure for Making AC

3.4 Characterization of Activated Carbon

Activated carbon that has been prepared has the following distinguishing characteristics:

3.4.1 Proximate analysis of EL:

According to ASTM, proximate analysis is the process of identifying moisture, volatile matter, ash, and fixed carbon using specific procedures. Fixed carbon, volatile matter, ash content and moisture content calculated, in accordance with ASTM D1037 (1991).

3.4.2 Component characterization of analysis of EL

A. Hemicellulose content

A 250mL flask was filled with one gram of extracted dried Enset leaf before 150mL of 0.5mole NaOH was added. With distilled water, the mixture was boiled for three hours. After cooling, it was filtered and rinsed until the PH was neutral. Equation (3.6) was used to determine the amount after a constant weight residue was baked at 105°C.

$$\text{Hemicellulose content} = \frac{Ma - Mb}{Ma} * 100\,\% \quad (3.2)$$

Where Ma and Mb represent the sample's initial and final masses (in grams), respectively

B. Lignin content

In summary, 1g of EL powder and 15mL of H_2SO_4 were mixed and left to remain at room temperature for two hrs. Once, distilled water of 500 milliliters added, the mix was heated for three hrs to take out the lignin that was insoluble, and then it was centrifuged (Song et al., 2019). The lignin was weighed once it had been dried in an oven. The amount of lignin was calculated with the help of equation (3.7).

$$\text{Lignin content (\%)} = \frac{Mf}{Mi} * 100\% \quad (3.3)$$

Where, Mi and Mf represent the sample's initial and final masses, respectively, in grams.

C. Cellulose content

It was calculated by deducting the total of hemicellulose and lignin from 100 and accounting for the constants of the other lignocellulose elements (Ayeni et al., 2018).

$$\text{Cellulose \%} = 100 - (\text{Hemicellulose} + \text{lignin}) \quad (3.4)$$

3.4.3 Elemental Analysis of the adsorbent

Elemental analyzer was used to carry out elemental analysis. That is, in order to determine the presence of components such as carbon, hydrogen, nitrogen, and other elements in the prepared EL AC sample.

3.4.4 AC yield

The amount of precursor that is changed throughout the carbonization process is indicated by the AC yield, which is the ratio of the precursor's final weight with its beginning weight. The following formula was used to get the yield (%) of AC:

$$\text{Yield (\%)} = \frac{W1}{W2} * 100\% \quad (3.5)$$

Where, W_2 is the weight of carbon generated by pyrolysis (dry basis) and W_1 is the weight of enset, which is used as a raw material to create carbon.

3.4.5 Zero charge point (PH_{PZC}) of AC

Michael et al. (2016) described the method to obtain the PH_{PZC}. When there are equal amounts of positive and negative charges on an AC surface, the aqueous solution PH level reached Eight. 0.1M NaCl solutions were made with PH initial (PH_i) values ranging from 2 to 12 in order to accomplish this. Next, a 0.1M solution of HCl or NaOH was added to these solutions to adjust their PH. After adding 0.1g of AC to 30mL of each solution, the mixtures was constantly stirred for 24hours at room temperature, or until stabilized PH obtained and was recorded as PH_f. The

intersection of the graph with the line with equation Y = f (X), which is the bisector of the first quadrant, was depicted by drawing the graph $PH_f = f(PH_i)$ is results PH_{PZC}. The PH of various solutions was determined using PH meter.

3.4.6. Iodine Number:

It refers to quantity of iodine that, at precisely 0.02N equilibrium iodine concentration, 1 g of activated carbon may absorb from a 0.1N iodine solution. One measure of activated carbon's micropore density is its iodine number. Micro porosity is increased in a sample with a higher iodine value. ASTM D4607-94(2006) provides a standard procedure for figuring out the iodine number of activated carbon.

$$\frac{X}{M}=\frac{(N1*126.93*V1)-\left[\frac{V1+VHCL}{VF}\right]*(NNa2S2O4*126.93*V\,Na2S2O4)}{M} \quad (3.6)$$

Where, V_1 = 25ml of iodine solution, $V_{Na2S2O4}$ = 10ml of sodium thio-sulfate solution used for titration, V_F = 10ml of filtrate used for titration, M = weight of activated carbon = 0.1gm, M_i = molar weight of iodine = 126.9044g/mol, and C_i = 0.045N = concentration of iodine solution.

3.4.7. Thermogravimetric analysis(TGA)

In order to assess the thermal materials behavior, thermogravimetric analysis (TGA) was performed by a thermal analyzer. The thermo balance automatically calculates the sample's weight loss based on temperature and time. The samples were heated at a rate of 20 oC per minute while 35ml of N_2 was flowing through them. Hu and colleagues (2008), Basta et al. (2008)a, and Kalderis et al. (2009).

3.4.8. Scanning electron microscopy (SEM) analysis

The SEM analyzer helps to investigate the morphology of AC surface. The precursors were layered using an apparatus of gold sputtering by gold to guarantee their conductivity and transparency. The coated sample was then stored in a sample container in favor of investigation (Somasundaram et. al., 2013Rosas et al., 2019).

3.4.9 Fourier transform infrared (FTIR) spectroscopy analysis

FTIR analyzer used to determine the functional group on the surface of the precursor. Prior to usage in infrared research, a specified precursor was combined with KBr crystals and shaped into a pellet. The uniformly shaped pellet inserted into the infrared test container for investigation.

Using a resolution of 2 cm-1, the Fourier transform infrared spectra of several materials were recorded between 400 and 4000cm-1 (Liu et al., 2019).

3.4.10 Surface area and pore size analysis

The surface areas of the samples were calculated by the ratio of pressure of the system (P) to initial pressure (Po) at 1 bar (i.e: P/ Po) by means of N_2 adsorption isotherm data using BET method.The average pore diameter and micro pore volume were calculated using the Dubinin-Radushkevich method (Ang et al., 2018). Gas adsorption analyzer was used to obtain samples' average pore size and surface area. Before the samples being measured (at a temperature of 200ºC and for three hours) in a vacuum, it became degasified. At 77.35K and adsorption equilibrium time of 60 seconds, the nitrogen adsorption-desorption measurements were collected for liquid nitrogen.

3.5 designing of the experiment

The three components with BBD (Box-Behnken experimental design) were used to analyze data of experiment for the fabrication of AC using RSM and Design-expert 12.0.0 software. Based on the outcomes of the experiment, ANOVA or analysis of variance was performed to model the relationship between various factors and the responses. The independent variables with the levels of examination listed in Table3.1.

Table3.1 Levels and independent variables

Independent variables	Unit	Level		
		Low	Medium	High
Temperature	ºC	400	500	600
IR	-	0.5	1	1.5
Holding Time	min	30	60	90

3.6 Batch Adsorption

3.6.1 Preparation of Phenol standards

To make a stock phenol solution, 1g of phenol was diluted with 1000ml of deionized water to make a solution containing 1g/l of phenol. To create the intermediate solution, 25ml of the stock solution were diluted with 250ml of de-ionized water to produce a phenol solution containing 100 mg/l. Standard solutions were made by adding 100 ml of de-ionized water to 10, 20, 30, 40,

and 50ml of intermediate solution, respectively, to get 10, 20, 30, 40, and 50mg/l of phenol solution.

3.6.2 Batch experiment

Numerous factors, for instance PH, adsorbent dose, contact time, initial concentration of phenol, and adsorbent dosage, have a substantial impact on adsorption capability (Mehta & Gonawala, 2014). To study the effects of various factors, batch adsorption experiments were performed. In a conical flask of 250ml volume, 0.1 g of the adsorbent with different phenol concentrations (10 to 50mg/l) of 100ml was combined. For 90 minutes, at room temperature, at 150rpm the combination stirred and swirled (Aremu, 2019). At intervals of 10, 20, 30, 60, 90, 120, and 150minutes, 3 to 4ml of samples were taken out of a 5ml and centrifuged at 3000rpm for 20minutes. By decantation and filtering, the supernatant solution was removed from the centrifuge. Each time the filter was used, it was backwashed with 50 ml of deionized water. The adsorbents weighing 0.2, 0.3, 0.4, and 0.5 grams were treated in the same way as previously mentioned. This investigation's perfect working conditions allowed the aforementioned technique to be used at pH levels of 2, 4, 6, 8, and 10. By dropping in to the solution either NaOH or HCl the PH was adjusted (2008) Rahman & Hameed. For the above-described technique, the adsorption process temperature was 25 °C at the optimal operating conditions established by this study.

3.6.3 Removal efficiency and adsorption capacities determination

Using UV spectrophotometer from the filtrated sample the amount of phenol in each sample's was measured. It was found that phenol has the maximum absorbance at a wavelength of 270 nm. This aligns with the conclusions drawn from the literature by Shri and Vijayababu (2020) as well as Girods et al. (2019). Priorly, a calibration curve which is linear over the concentration was constructed.

A.**Adsorption Capacities**

For each sample, at a given time (t) the adsorption capacities (q_t) were calculated using equation (3.11), which was derived by Li et. al. (2019).

$$q_t = \frac{(Co - Ct)v}{m} \tag{3.7}$$

Using equation (3.12),for each experimental batch the equilibrium adsorption capacity qe was determined following the recommendations of Demibras et al. (2009) and Karaca et al. (2008):

$$q_e = \frac{(Co - Ce)v}{m} \quad (3.8)$$

B. **Adsorption Removal Efficiency**

According to Garg et al.'s (2008) suggestion, equation (3.13) was used to calculate the adsorption removal efficiency.

$$RE = \frac{(Co - Ce)}{Co} * 100\% \quad (3.9)$$

Where: = initial solute concentration (mg/L), volume of solution (L), mass of solute at equilibrium (mg/L), mass of solute at time t (mg/L), adsorption capacity at equilibrium (mg/g), and removal efficiency (%) all occur.

3.6.4 Adsorption equilibrium isotherm study

The experimental results for the equilibrium isotherm research were examined using the isotherm models that have been published in the literature.

A. Parameters of Langmuir Isotherm

The graph below plots against the linearized isotherm model of Langmuir. Based on the intercept and slope of the plot, equation (3.14) was utilized to get the equilibrium isotherm parameters for the model (Amin, 2008; Homagai et al., 2010)

$$C_e/q_e = \frac{1}{(bQm)} + \left(\frac{Ce}{Qm}\right)$$

(3.10)

Where Q_e is the adsorption capacity at equilibrium (mg/g), Qm is the maximal monolayer adsorption capacity (mg/g), b is the Langmuir isotherm constant (dm3/mg), and C_e is the equilibrium concentration of solute (mg/L).

B. Freundlinch Isotherm Parameters

linearized isotherm model form of the Freundlinch, which is displayed below, was used for the plotting against. Based on the intercept and slope of the plot, equation (3.15) used to get the models' parameters of equilibrium isotherm, as reported by Krishnan et. al. (2011) and Gunduzoglu (2010) were utilized.

$$\log q_e = \log K_f + \left(\frac{1}{n}\right) \log C_e \quad (3.11)$$

Where: Ce = equilibrium solute concentration (mg/L), qe = adsorption capacity at equilibrium (mg/g), Kf = Freundlich isotherm constant (mg/g), and n = adsorption intensity.

3.6.5 Adsorption kinetic study

To assess data of the experiment for the adsorption kinetic investigation, the following kinetic models which described below were employed.

A. Model pseudo-first order

On bases of adsorption capacity of solid Lagergren developed a model for a rate expression first order kinetics and presented below:

$$\log q - \left(\frac{K1t}{2.303}\right) = \text{Log}(q - q_t) \quad (3.12)$$

Where = k1 is the equilibrium rate constant of the pseudo-first-order adsorption (min–1) and qt is the adsorption capacity at time t (mg/g).

B. Model Pseudo-Second-Order

linearized model of pseudo-second-order which is displayed below, was used for the plotting against. To evaluate parameters of kinetic model, the intercept and slope of the plot of equation (3.16) were used (Kaouah et al., 2013).

$$t/q_t = \left(\frac{1}{k2qe2}\right) + \left(\frac{1}{qe}\right)t$$

(3.13)

Where= q_e is the adsorption capacity at equilibrium in (mg/g), q_t is the adsorption capacity at time t (in mg/g), k_2 is the kinetic rate constant in (mg/g*min), and t is the time (in min).

3.6.6 Experimental design

Variables like temperature, adsorbent dosage, PH and initial phenol concentration were taken into account in order to create the experimental matrix. The uncoded measurement units needed to convert into coded for evaluating the design factor. Each levels of factor represented by the codes +1 (high) and -1 (low). The phenol removal efficiency (RE %) was provided as the response. The trial runs were conducted using the available AC5 samples. To analyze and generate experimental matrix, a statistical tool Design Expert 12.0.0 was used in order to assess the effects of different factors on phenol removal capacity. The factors' ranges and numbers investigation were shown in table 3.2 below.

Table3.2 factorial design levels and ranges

Independent variables	Coded symbol	Range and level	
		Low(-1)	High(+)
PH	A	2	10
Initial conc.(mg/l)	B	10	50
Adsorbent dose(mg/g)	C	0.1	0.5
Temperature (°C)	D	20	50

4. Result and discussion

4.1. Enset leaf AC Characterization

4.1.1 Componential and proximate and analysis

Any carbonaceous substance, both organic and inorganic, can be used to make activated carbons (ACs). However, the choice of conveniently accessible and affordable feed stocks is determined by process economics. Biomass precursors offer the most economical service because of their high hardness, low mineral content, and renewable nature.

There is a ton of literature on the usage of lignocellulosic materials like nutshells and plum stones. The preparation of AC using enset leaf, on the other hand, got far less attention. Table 4.1 provided information on the chemical make-up of EL as well as their varied physical characteristics. The results show that the EL has low lignin content (10.3%) and a high cellulose concentration (18.4%), which are essential qualities for the synthesis of AC. The EL has 8.35% moisture content, a 71.09% volatile matter content, a 3.28% ash content, and 17.28% fixed carbon content, according to the Proximate study. The results show that EL has a lower proportion of ash and a higher proportion of volatile matter and, making it an excellent initial material for the production of AC. A biomass resource with a low ash level and high volatile matter content is a great precursor for creating AC, claims the Faculty of Health and Life Science of Malaysia (2022). The last investigation shows the sample has a high oxygen and carbon content but low nitrogen and sulfur content.

Table 4.1 Analytical comparison of the composition and characteristics of EL and agricultural waste

Property	**Enset leaf**

Lignocellulose composition	
Cellulose	**18.4**
Lignin	**10.3**
Hemicellulose + Others	**71.3**
Proximate analysis	
Moisture	**8.35**
Volatile Matter	**71.09**
Fixed Carbon	**17.28**
Ash	**3.28**
Ultimate Analysis	
C	**44.76**
H	**5.89**
N	**0.77**
S	**0.05**
O	**48.53**

Agricultural waste	**Proximate Analysis**			**Ultimate Analysis**					**Lignocellulos composition (%)**		
	M.C	A.C	V.C	**C**	**H**	**N**	**S**	**O**	**Cellulos.**	**Hemicellu.**	**Lignin**
Banana peel	11.56	9.28	88.02	35.6	6.19	1.6	20.7	45.9	-	-	-
Bamboo	15.3	1.76	70.12	34.4	4.61	0.2	0.07	-	26	15	21
Cassava peel	14.00	4.5	59.4	59.3	9.78	2.0	0.11	28.7	37.9	23.9	7.5
Coconut shell	8.21	0.80	77.82	49.6	7.31	0.22	0.10	42.75	14.0	32	46.0
Cotton stalks	6.00	6.3	70.5	43.6	5.8	0.8	0.00	49.8	80.9	5.20	-
Rice husk	6.34	16.7	67.5	36.5	4.82	0.8	-	41.1	30.4	28.03	36.0
Sugar BG	8.61	4.05	86.02	47.3	6.2	0.2	-	44.1	42.1	36.0	19.3

https://doi.org/10.3390/w14203203; Malaysia Water 2022, 14(20), 3203

4.1.2 Thermo gravimeter analysis (TGA)

During the TGA, the N_2 environments kept at a temperature ranged from 25 to 900°C and constant heating rate of 10°C/min. When it comes to raw materials, the initial stage's moisture release and surface-water bound is responsible for 12.842% of the weight loss between 27 and 246 degrees Celsius. The remarkable 41.62% weight loss was observed within the temperature range of 250°C to 351°C. The main reason for the weight loss is the degradation of low molecular weight furan derivatives and cellulose. Because hemicellulose and lignin are breaking down above 350 degrees Celsius, there is a consistent and continual loss of weight up to 850 degrees Celsius. As a result, the range of 400 to 600 degrees Celsius and the duration of 30 to 90 minutes are the parameters for the carbonization temperature in this investigation.

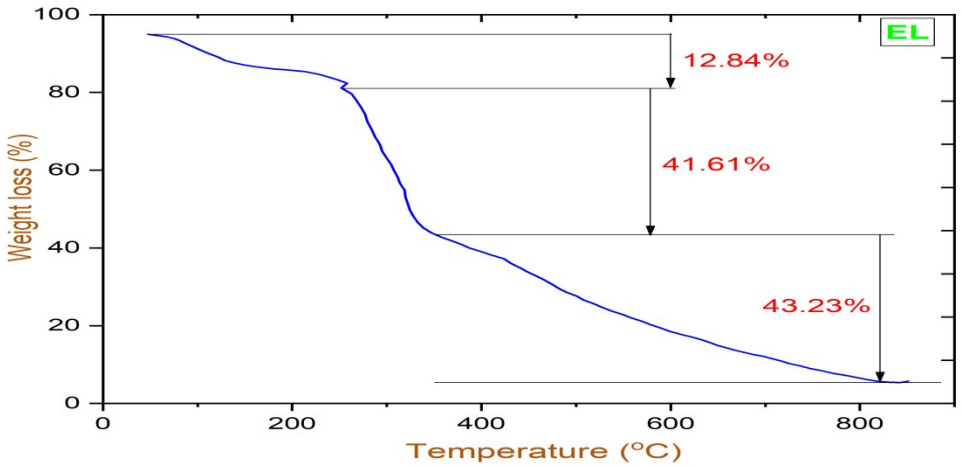

Fig. 4.1 TGA for raw EL

4.1.3. FTIR analysis

In order to determine the prepared AC bonds, FTIR analysis used as it show in the Fig.4.2 below. Since the bonds were either created during the activation process or were present in their ancestor EL, their discovery was expected. Even though the occurrence of chlorine in the AC was unwanted, it suggests that a temperature over 235°C should be reached during carbonization in order to eliminate all chlorine from the produced AC precursor. The FTIR analysis graph is shown below:

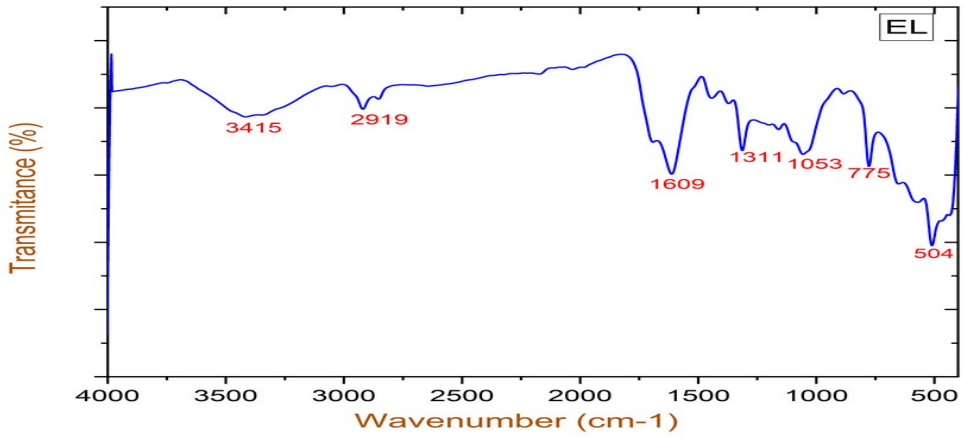

Fig. 4.2: FTIR result for AC_5

For chemically treated EL AC_5 to verify the functional groups vibration frequency of FTIR spectra were used. On the AC, the peaks were intense and quite high. These peaks showed notable absorption bands at different frequency ranges. The measurement range for the adsorbent's spectrum was 400–4000cm-1 wave numbers. All of the spectra, as seen in Fig. 4.2 above, include peaks' of the absorption at 3488 and 1020cm-1, which is mainly indicative of the vibration band of stretching of the O-H (hydrogen bond) in phenols, alcohols, and carboxyl from AC, as well as band of C-H. The primary band in the AC, which is visible between 3450 and 3500cm-1, is caused by the moisture content of the sample. Because of the preexisting methyl groups of C-C stretching, there is a peak at 2430 and 2919cm-1. The amine functional group N-H bending and stretching must result in FTIR bands that are observable between 1616cm-1.The complete carbonization of the EL is evident from the absence of these bands in the leaf's activated carbon spectrum. Wave numbers 1312cm-1 were caused by a hydroxyl molecule. The aromatic C-H vibrations result in the peak located at around 775cm-1. A compound's aromatic bending modes are represented by wave number 650cm-1. Wave number 511cm-1 shows the para replacement of the benzene rings. The FTIR spectra indicate the adsorption affinity of each functional group (Prahas et al. 2019).

4.1.4 SEM analysis

The non-consistency in the sizes, shapes, and architectures of the particles were determined by SEM images. It's also utilized to observe the development of the pores. It's also utilized to observe the development of the pores. In this instance, the preparation and characterization of the

AC was the sole focus of the study, despite the fact that numerous images offer a more comprehensive perspective of the effects of various parameters on the prepared AC. The images show the wide range of sizes and shapes that make up the distribution of AC particle size. The surface of the AC particles is also extremely rough, and they are piled one on top of the other, much like sponges. The results of the examination into the surface topography of ACs and raw EL are shown in Fig. 4.3.

Fig. 4.3 SEM result of (a) Raw Enset leave, (b) AC_1, (c) AC_5 and (d) AC_8

As shown in Figure 4.3(a), the raw's surface is smooth yet devoid of cavities. The three active surfaces have little pores visible on them. The raw EL sample's passage structure is essential for the production of AC. The channel allows the chemical activation ingredient to be absorbed by the EL powder and start the pore creation process.

Sample AC_5's surface morphology exhibits comparatively more well-structured pores at 500°C carbonization temperature and 1.0 hour activation time, as Figure 4.3b illustrates. In contrast, at 400°C carbonization temperature and 60 minutes activation time, Figure 4.3b shows slightly broken porous walls. The result of assuming excessive heat during carbonization at 600°C for one hour is shown in Figure 4.3d. This implies that the sample is being overheated at 600°C, which is why the porous formation is knocking and breaking (Kamil, 2019). Furthermore, an excessively protracted carbonization period exacerbates the synthesis of AC. H_3PO_4 activation led to the development of extra carbon surfaces on AC_3, AC_5, and AC_8 in addition to the previously stated variables. This variety can be attributed to the diffusion of molecule of H_3PO_4 into the pores, encouraging the expansion of the carbon-H_3PO_4 reaction through processes of acid hydrolysis that could subsequently lead to the formation of further pores. The macro pores

and apparent irregular holes in ACs are present (Elkady et al. 2018). The findings imply the surface porosity of synthetic ACs may allow for a variety of applications.

4.1.4 Iodine Number (I.N)

The average I.N of commercially produced AC is greater than 1000. It is commonly recognized that as I.N rises, so does the adsorption capability. Iodine numbers of 500 to 1200 are generally indicative of high-quality activated carbon (Elkady et al. 2018). The table below provides the appropriate number of iodine in activated carbons.

Table 4.2 I.N of ACs

Sample	$A.C_1$	$A.C_2$	$A.C_3$	$A.C_4$	$A.C_5$	$A.C_6$	$A.C_7$	$A.C_8$	$A..C_9$
I. N (mg .g -1)	261	419.98	515.34	778.61	982.64	838.63	711.36	727	715.57

The generated ACs for $A.C_3$, $A.C_4$, $A.C_5$, $A.C_6$, $A.C_7$, and $A.C_9$ have iodine numbers that suggest adequate adsorption capacity as well as acceptable micro pore network development. It has been noted that the prepared activated carbon's surface area per unit gram may be approximately determined by the I.N. As a result, the produced activated carbon iodine number ranging from 200-850 mg/g is about equal to surface area, with a little margin of error.

4.1.5 Porosity and Surface Area Analysis

Table 4.3: Porosity and Surface area selected samples results

Sample	Activation Time (min)	IR	Carbonization Temperature (°C)	SBET (m^2 /g)
$A.C_1$	30	0.5	400	265
$A.C_4$	30	0.5	500	812
$A.C_7$	30	0.5	600	742
$A.C_2$	60	1	400	432
$A.C_5$	60	1	500	1023
$A.C_8$	60	1	600	759
$A.C_3$	90	1.5	400	524
$A.C_6$	90	1.5	500	875
AC_9	90	1.5	600	730

Under different techniques of preparation the generated EL AC pores' surface area formed showed in the above table. From the above data, the lowest carbonization temperature for EL AC is 400°C, and above 600°C temperature fallout in less than optimal performance. With the exclusion of sample $A.C_3$, which is carbonized for 30 minutes at 400°C, $A.C_1$, $A.C_2$, and $A.C_9$ are carbonized at 400°C and 600°C, correspondingly gives a significantly elevated SBET. But samples $A.C_4$ up to $A.C_8$ encompass elevated SBET than the others. Raising the H_3PO_4 impregnation ratio and carbonization temperature typically causes pore widening. Carbon gasification improvement with higher H_3PO_4 ratio increases the porosity and pore size of AC. Raising the temperature of carbonization causes a direct increase in the rate of the C-H_3PO_4 reaction and a subsequent rise in carbon burn-off. H_3PO_4 is a strong acid that can accelerate the rate of dehydrogenation and oxidation carbon atoms at the interface with promoting the raise in production of additional tar and porosity (Mopoung, 2018). According to results comparing samples $A.C_5$ and $A.C_6$ increased H_3PO_4 activation ratio is also not recommended for, since it impacts the lower impregnated ratio than the efficiency of pore formation with a smaller surface area. The enormously micro porous AC transforms into a new form where the meso pores take control of the entire pore size distribution when the amount of activating agent is surpassed (Karatepe, 2019). Once the application of impregnation goes above the maximum value, there will be a considerable transfer in developments of pore size because of the lignocellulosic contents react with elevated symphony of potassium, through impregnation phases in addition to activation (Yauvz, 2018).Furthermore, the pore growth promoted by quantity of a dehydrating agent increases more as the impregnation ratio increases. Fortunately, pore formation once more hindered when the limit is exceeded (Liv & Bao, 2020). Lastly, it has been shown that the mesoporous pores are the most present in all of the samples analyzed. According to SBET, sample AC5, which measures 1023 m2 per gram and has sub-microporous group pore sizes of 1.682 nm, generates the greatest surface area based on the data. Since sample AC5 produced the best results out of all the samples, it was utilized to assess the phenol's adsorption capacity.

4.1.6 Distribution of pore size

The distribution of pore size of AC_5 synthesized under ideal conditions was calculated using the Dubinin-Astakhov (DA) equation; the outcome is shown in Fig.4.6. The figure was used to calculate the average diameter of the micropores in the adsorbents, which is 1.71 nm.

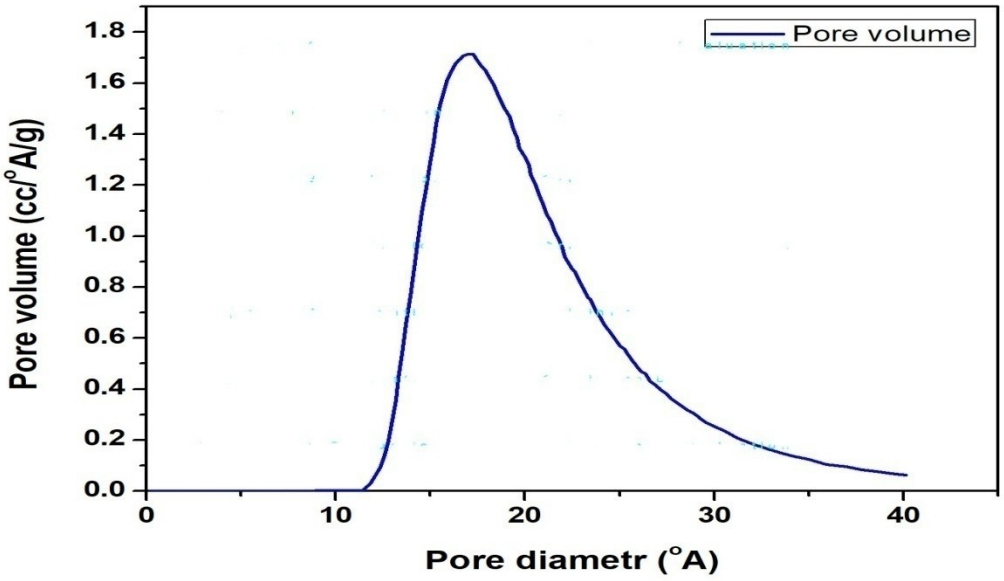

Fig.4.6 pore size distribution

4.1.7 Point of Zero charge (PHpzc)

PHpzc is the state when the adsorbent surface is devoid of any electric charge. This experiment employed the solid addition method. 12 flasks with 0.1g of adsorbent each were then filled with 0.01M (50mL) of NaCl solution. A PH meter is used to determine the solutions PH, ranging from 2 up to 12. As the PHpzc is higher than the solution PH, the adsorbent surface becomes charged negatively, and when it is lower than PHpzc, it becomes charged positively (Temesgen et. al., 2018). This directed that penol's basic regions were most likely being bound by the adsorbent that was created. The next step became plotting the results "PH final versus PH initial". The junction of "PH final versus PH initial" curves, or approximately 7.9, is the adsorbent point of zero charge. Fig.4.7 shows the graph of PH_i vs PH_f.

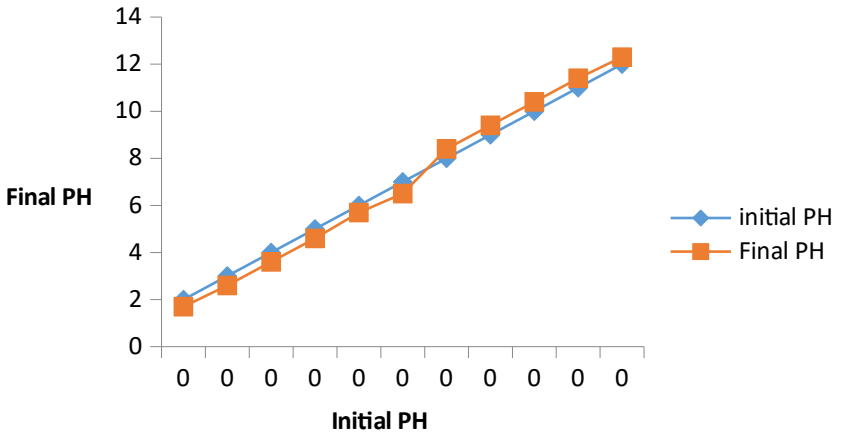

Figure 4.7 Plot of PH initial versus PH final for determining PHpzc

4.2 Activated carbon Enset Leaf

When making activated carbon (AC) chemically, the porosity development is dependent on several process variables, such as the carbonization temperature, holding time, and impregnation ratio.

4.2.1. AC yield

Based on formation of pore structure, and the surface chemistry, impacts of activation temperature and the impregnation ratio on the activation process were investigated. In Figure 4.8 EL ACs yields are displayed together with the effects of H_3PO_4 impregnation ratio and the activation temperature.

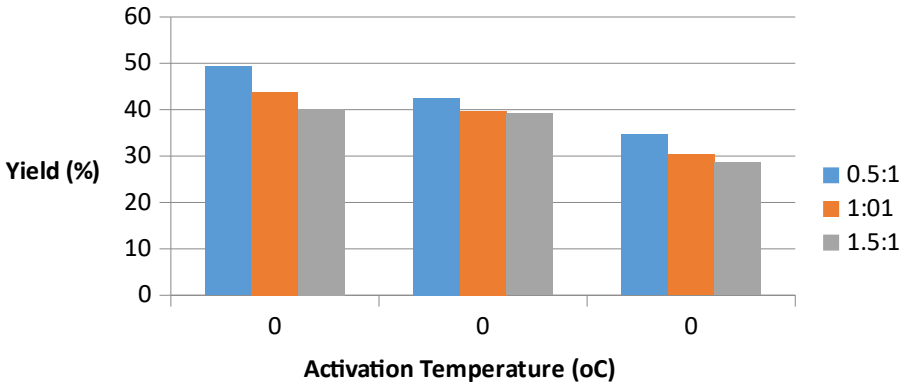

Fig. 4.8: yields of the ACs derived from Enset leave by H_3PO_4 activation

4.2.1.1. Effect of Activation Process Variables on ACs yield

(a)Effect of Impregnation on ACs Yield

ACs yield determined by dividing final activated carbon's weight by the dried Enset leaf's weight. The effect on AC yield was investigated by varying the carbonization temperature values (400, 500, and 600ºC) and at different impregnation ratio (0.5, 1 and 1.5). As is often recognized, the process of conversion of carbon from lignocellulos materials involves the release of CO_2, H and O atoms, CO, CH_4, H_2O, tar or aldehydes. Yield of carbonization is determined by the carbon quantity eliminated by interaction with H and O atoms (Caturla et. al., 2021). When Enset leaves are carbonized at 400°C without being impregnated with H_3PO_4, a higher AC yield of 49.30% is obtained. Figure 4.9 shows the impact of impregnation ratio on the preparation of activated carbon during activation. At 0.5 and 1.5 impregnation ratios, the maximum and minimum yields for H3PO4 impregnation were obtained, which were 49.3% and 28.6%, respectively. The results displays at 400 and 600ºC respectively, as the impregnation ratio increases from 0.5 to 1.5, the yield decreases continuously from 39.72% near 24.98%. As the impregnation ratio is raised, more volatiles are released from the sample, which results in a yield decline. Qian et al. (2019) suggest that the reason for the lower yield seen with increased impregnation could be related to the inclusion of an activating agent to enhance carbon burn-off.

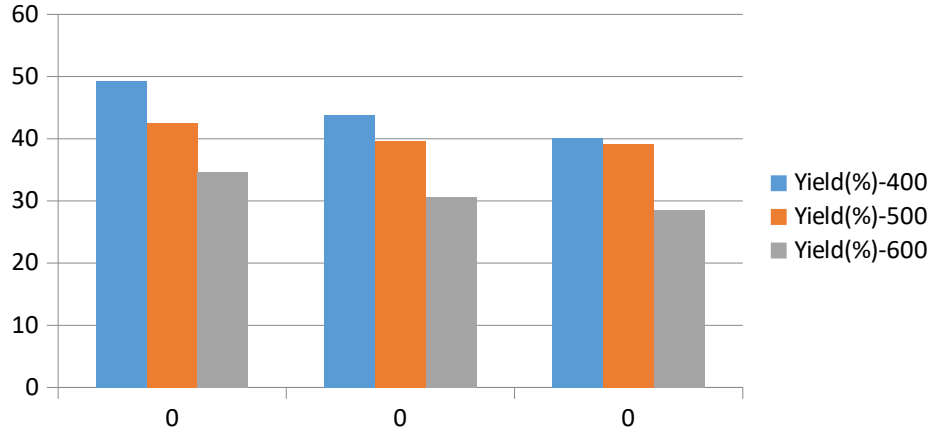

Figure 4.9: impregnation ratio impact on yield of EL AC

(b) Temperature effect on EL AC yield

The ultimate activation temperature, an important component in the manufacture of AC, greatly affects the yield and porosity characteristics. A number of authors (Wu et al., 2017) investigated how the temperature of carbonization affected the synthesis of AC using different precursors. The results showed, the ACs yield had a substantially influenced by activation temperature. A higher activation temperature results in a lower carbon yield because of a considerable drying of the carbonaceous structure of the precursor.

Figure 4.10 illustrates activation temperature impact on ACs yield. The result showed that as the activation temperature climbs from 400°C to 600°C, the ACs yield decreases for all samples. Higher temperatures enhance the catalytic activity of phosphoric acid, causing the dehydration and breakdown of biomass to occur more quickly. This releases volatile chemicals from ensilage and lowers the output of activation carbon. Fig. 4.1 shows that as the carbonization temperature increased from 500°C to 600°C, ACs yield decreased dramatically. There was a little decrease in yield when the carbonization temperature increased from 400 to 500°C. The main reason for this is that warmer temperatures promote tar volatilization and carbon burn-off (Adinata et al., 2017). The yield of generated AC_5 decreased from 49.3% to 27.28% when temperature of carbonization rose from 400 to 600°C.

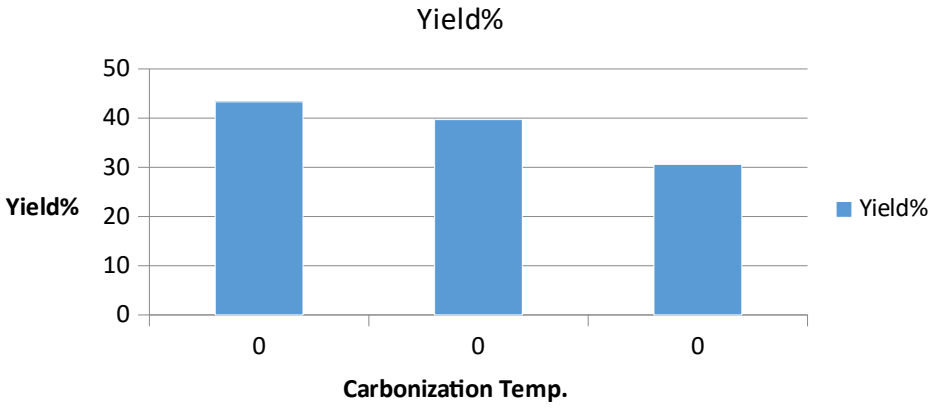

Fig. 4.10: carbonization temperature impact on the ACs Yield

(C) Effect of Holding Time on Yield of AC

Holding Time's Impact on AC Yield In order to prepare AC samples under ideal conditions for the carbonization temperature and impregnation ratio, several holding times (30, 60, and 90 min) were used. Figure 4.9 illustrates the manufactured ACs yields affected by holding time. As the holding period was increased (30 to 90 minutes), the percentage of yield gained decreased. Longer holding times resulted in a lower yield due to increased burn-off carbon (Qian et. al., 2017). The produced AC_5 yield decreased from 42.5 to 39.2% as holding time increased from 30 to 90 minutes. More volatiles might have been released if the sample had been kept at the ultimate carbonization temperature for a longer amount of time.

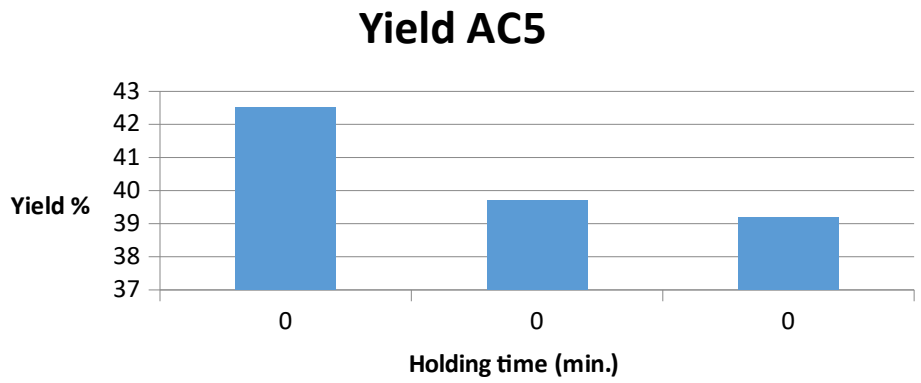

Figure4.11 holding time effect on EL AC Yield

4.2.2 ACs Surface area and porosity

Porosity and surface area of AC is defined by its pore volume and surface area. According to Erdem et al. (2018), high-quality activated carbons are estimated to need between 0.2 and 0.6 cm^3 of total pore volume and 800-1500 m2 of surface area per gram. An examination was conducted into the impregnation ratio and activation temperature impact on several porosity parameters, such as surface area. Pore volume and specific surface area of the EL ACs which activated by the temperatures (400, 500, and 600°C) and with H_3PO_4 at different impregnation ratios (0.5, 1, and 1.5) and are summarized in Table 4.5 based on the N_2 isotherms at 77K. Specific surface area at a relative pressure in the P/P0 = (0.05–0.35) range was calculated from the adsorption branch based on the BET (S. Liu et al., 2019).

4.2.2.1 Activation Process Variables effect on AC BET Surface area

(a) Carbonization temperature effects on BET Surface area

Within the temperature range of 400 to 600°C, at impregnation ratio 1 and holding period 60min was investigated the impact activation temperature on pore volume and surface area. Pore volume and specific surface area of the ACs were influenced by the activation temperature, as seen in Fig. 4.13. The surface area of ACs increased from 524m2 g-1 to 1023m^2 g-1 as the activation temperature from 400°C to 500°C .Pores were formed because of the intense heat effect (up to 500°C) on the volatile matter contents. H_3PO_4 at low temperatures (approximately 400°C), glycosidic linkages hydrolyzed in cellulose, hemicellulose and cleaves aryl ether bonds to catalyze a variety of changes in lignin, such as, degradation, condensation, and dehydration. Jagtoyen and Derbyshire (2016) claim that these reactions promote the evolution of increased porosity at low temperature by releasing CO_2, CH4, CO, and H_2O. Therefore, it was found that

500°C, which had a 0.45cc/g of pore volume and 1020m^2/g of high surface area, was optimal activation temperature. ST and VT progressively dropped as the temperature of pyrolysis increased. Pores were formed because of the intense heat effect (up to 500oC) on the volatile matter contents. At low temperatures (approximately 400oC), hydrolyzed phosphoric acid glycosidic linkages in cellulose, hemicellulose and cleaves aryl ether bonds to catalyze a variety of changes in lignin, such as dehydration, degradation, and condensation.

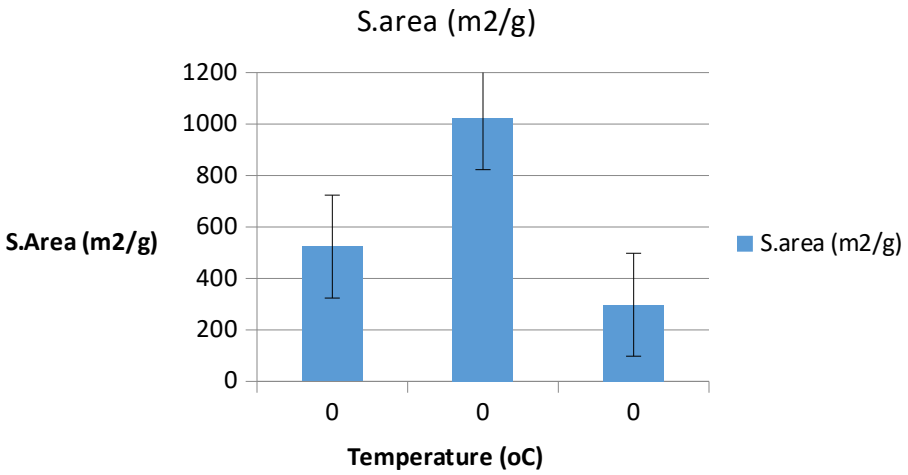

Fig. 4.12: Activation temperatures effect on surface area of EL AC

(b) Impregnation Ratio effect on BET

Micropore volume and surface area had shown a growing tendency with an increase in H_3PO_4 impregnation, and an opposite trend with an increase in impregnation concentration. Tar is released by ACs formed by H_3PO_4 activation at lower temperatures, and this effect becomes more apparent when H_3PO_4 is at larger degrees of impregnation. Tar fills the interspace of the sample and act as a binder. It gives mechanical firmness and a intense micro porous structure and on carbonization the release increased (Rosas et. al., 2015). The sample produced by impregnation with 1:1 H_3PO_4 and carbonized at 500°C for a one-hour holding period produced 0.45 cc/g of micro pore volume and 1023 m^2/g largest micro pore surface area. The concentration of H_3PO_4 at which to impregnate the precursor to induce the development of microporosity was shown to be optimal at 1:1. The surface area decreased to 604 m^2 g-1 (Fig. 4.13) as the impregnation ratio increased from 1 to 1.5. The result might be some pores collapsing and some enlarging at higher impregnation ratios. Taking into account impregnation 1:1 ratio was chosen to produce AC from Enset leaf for various BET surface area.

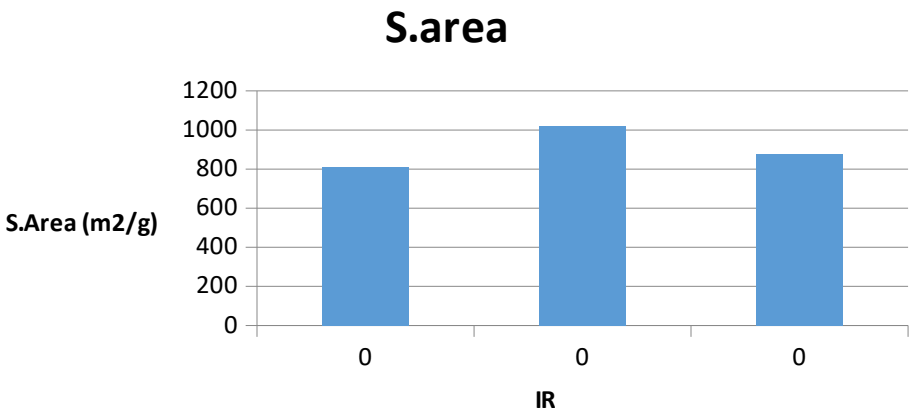

Figure 4.13 effect of I.R on surface area

(c). Holding time effect on pore volume and surface area

In conjunction with the final carbonization temperature, holding duration and impregnation ratio was major porous structure formation factor. The change in ACs' pore volume and surface area at the final carbonization temperature, obtained from H_3PO_4 activation, is depicted in Figure 4.14 for a variety of holding times (30–90 min). The results showed that the pore volume and surface area values increased from 0.16cc/g to 0.65cc/g and 348m^2/g to 1023m2/g and, respectively, when the holding duration was increased from 30 to 60 min at 500°C. In addition to a range of holding times (30 to 90 min), the ideal sample preparation parameters (impregnation 1:1 and carbonization temperature, 500°C) were applied. As the holding time was increased beyond 60 minutes, pore volume and surface area reduced. According to Diao et. al. (2017), this implies that extended retention periods caused some reducing pore volume, surface area, and pores to expand.

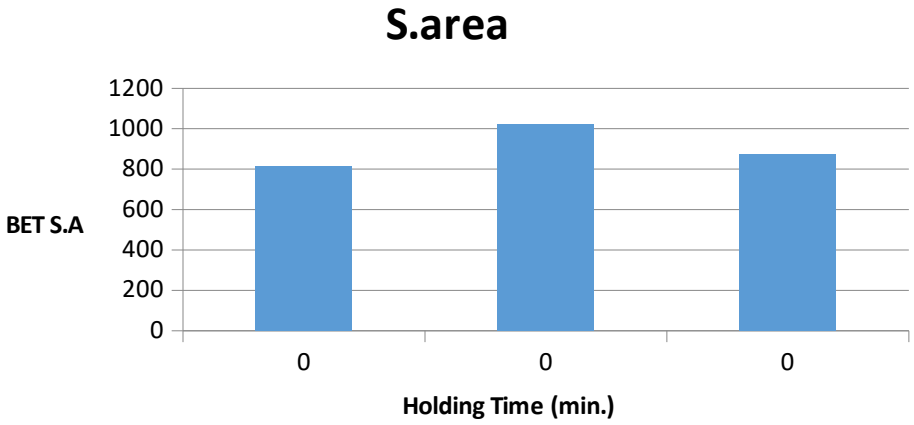

Fig. 4.14: Surface area and holding time effects

4.3 A statistical examination of the outcomes of the experiment

In this work, the effects of the activation time, impregnation ratio, and activation temperature on AC production were investigated by RSM based on BBD and Design-expert software 12.0.0. Table 4.4 displays the results of the ANOVA performed to assess the statistical significance of the model. (Where, temperature is B, time is H, and A is equal to I.R)

Table 4.4: EL AC Response Surface Quadratic Model: Analysis of Variance

		Factor1	Factor2	Factor3	Response1	Respons2	Response3
Std	**Run**	**A:I.R**	**B:Temperature**	**C:Holding time**	**BET S.area**	**yield**	**Iodine N.**
			oC	min	m2/g		
1	3	0.5	400	60	265.18	48.87	216
3	5	0.5	600	60	742.71	33.91	724
5	10	0.5	500	30	812.94	42.54	785
7	12	0.5	500	90	764.71	41.17	739
12	2	1	600	90	798.15	29.88	753
10	4	1	600	30	763	30.75	738
9	6	1	400	30	408.22	43.96	386
11	7	1	400	90	416.36	43.08	390
17	9	1	500	60	1023.32	39.73	982
16	11	1	500	60	989.64	39.69	956
14	14	1	500	60	988.63	39.77	951
13	15	1	500	60			
15	16	1	500	60			
6	1	1.5	500	30	875.66	39.32	862
8	8	1.5	500	90	846.79	39.24	830
4	13	1.5	600	60	759.05	28.69	718
2	17	1.5	400	60	524.07	40.35	503

Source	**Sum of Squares**	**df**	**Mean Square**	**F-value**	**p-value**	
Model	7.256E+05	9	80616.85	84.15	< 0.0001	significant
A-I.R	22053.15	1	22053.15	23.02	0.0049	
B-Temperature	2.625E+05	1	2.625E+05	273.98	< 0.0001	
C-Holding time	142.89	1	142.89	0.1491	0.7152	
AB	14707.63	1	14707.63	15.35	0.0112	
AC	93.70	1	93.70	0.0978	0.7671	
BC	182.39	1	182.39	0.1904	0.6808	

A^2	36622.77	1	36622.77	38.23	0.0016	
B^2	3.977E+05	1	3.977E+05	415.10	< 0.0001	
C^2	21277.69	1	21277.69	22.21	0.0053	
Residual	4790.16	5	958.03			
Lack of Fit	4010.58	3	1336.86	3.43	0.2339	not significant
Pure Error	779.59	2	389.79			
Cor Total	7.303E+05	14				

Based on F-value of 22.67 the model is deemed significant. Noise has a mere 0.44% possibility of producing a "Model F-Value" of this magnitude. The significance of the model terms suggested by "Prob > F" values less than 0.0500. In this instance A, B, A^2, and B^2 are important model terms. If the value is greater than 0.1000 the model terms are not significant. The "Lack of Fit F-value" of 3.43 suggests that there is no statistical significance between the Lack of Fit and pure error. A negligible mismatch is advantageous.

Table 4.5: The model's R-squared (R^2) value

Std. Dev.	1.29	**R^2**	0.9952
Mean	79.50	**Adjusted R^2**	0.9928
C.V. %	1.63	**Predicted R^2**	0.9877
		Adeq Precision	45.5145

0.9877 of "Pred R-Squared" value is as close to 0.9928 of "Adj R-Squared" value as one might normally expect. The design space can be used to navigate this model.

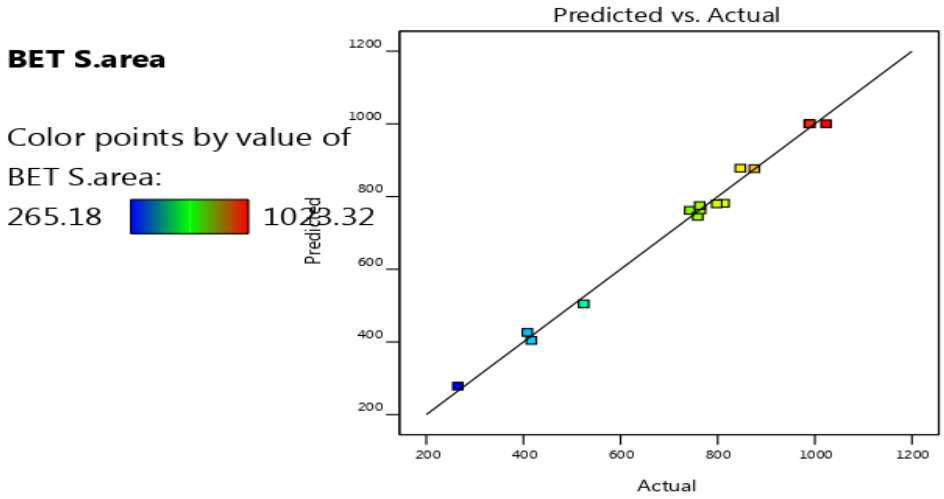

Fig. 4.15: Fitted mode diagnostic plot

The coded and actual components that make up the actual and predictive model are shown below. These terms are not suitable for modeling future response, but they can be used to regenerate the experiment's results. Finished Equation with Coded Factors:

BET S.area = 999.91+57.60 * A+147.64* B+ 5.31* C- 96.84 * A^2- 326.70 * B^2- 81.60 * C^2- 61.63 * A * B- 36.77* A * C- 41.25 * B * C

Final equation with actual factors:

BET S.area =-9921.23700+1653.32025 * I.R+36.20376 * Temperature+20.38422 * H.Time- 387.35950* $I.R^2$- 0.032670* $Temperature^2$-0.090670* $H.Time^2$-1.23268 * I.R *Temperature- 2.45107 * I.R * H.Time- 0.013751 * Temperature * H.Time

4.3.1 Activation Process Variables Interaction Effect on Surface Area of AC

4.3.1.1 Activation Temperature and Impregnation Ratio Interaction Effect

The collective effects of impregnation ratio and activation temperature on BET surface area AC_5 at constant holding time (60min) were shown using a 3D response surface plot (Fig. 4.16). The figure illustrates how the surface area improved by two settings. At a moderate impregnation ratio and activation temperature highest surface area achieved and indicated by red area on the the AC BET surface area plot. A BET surface area of 1023 m^2 g-1 was achieved at an impregnation ratio of 1:1and activation temperature of 500ºC.

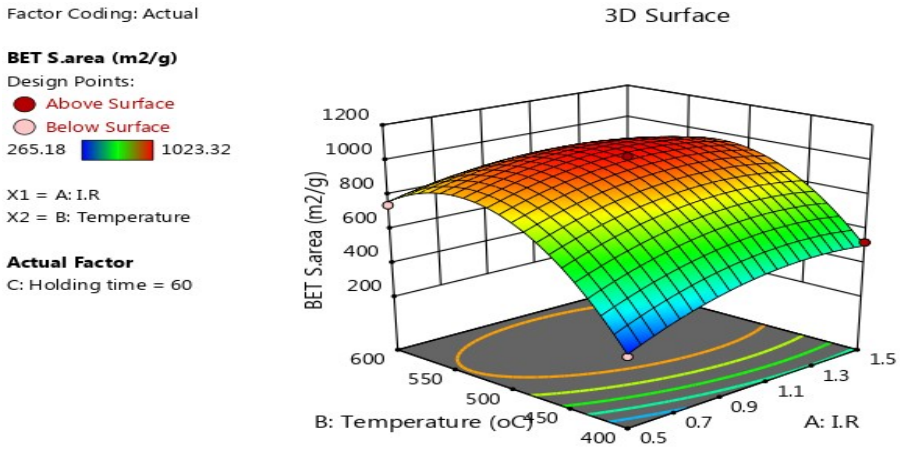

Fig. 4.16: temperature and impregnation ratio interaction effect on surface area AC surface 3D plot

4.3.1.2 Time and Activation Temperature interaction effect

Fig.4.18 which is the 3D surface response plot shows the activation duration and temperature interaction influence at 1:1 fixed impregnation ratio. As shown in the 3D plot, the dome-shaped

region shows the surface area of the AC experienced a lowest value at lower time and activation temperature and a highest rate at intermediate activation temperature and time. The surface area generated less when both components were more important.

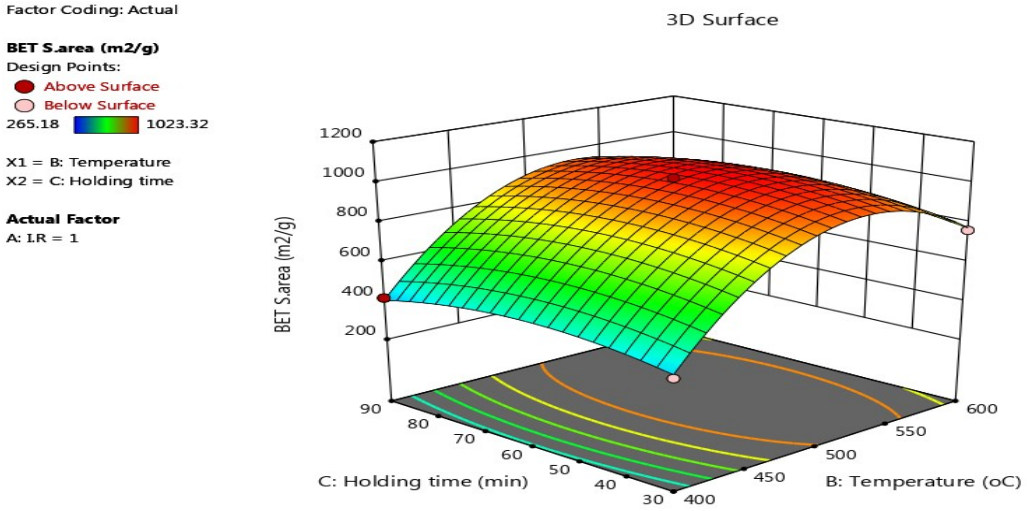

Fig. 4.18: Interaction Effect of Impregnation Ratio and Time

4.4 Adsorption of phenol

Because the produced activated carbon samples are made of highly porous materials, they can be utilized to extract organic pollutants from aqueous solutions, such phenol. Usually, a number of variables were changed to carry out the adsorption process, including the contact time, initial concentration, PH value, and adsorbent dose. The following conditions of adsorption were investigated as an adsorbent for the elimination of phenol to gain vastly effective carbon:

4.4.1 Standard calibration curve

To plot of known concentrations of phenol standard calibration curve, at maximum wavelength of 270nm absorbance was calculated. The calibration curve which is a linear fluctuation up to concentration of 100 mg/l constructed using UV spectroscopy. A greater quantities of phenol samples were using distilled water became diluted. The, which is, is shown in Figure 4.17 shows linear calibration curve of standard known phenol concentration utilized to determine the unknown quantity.

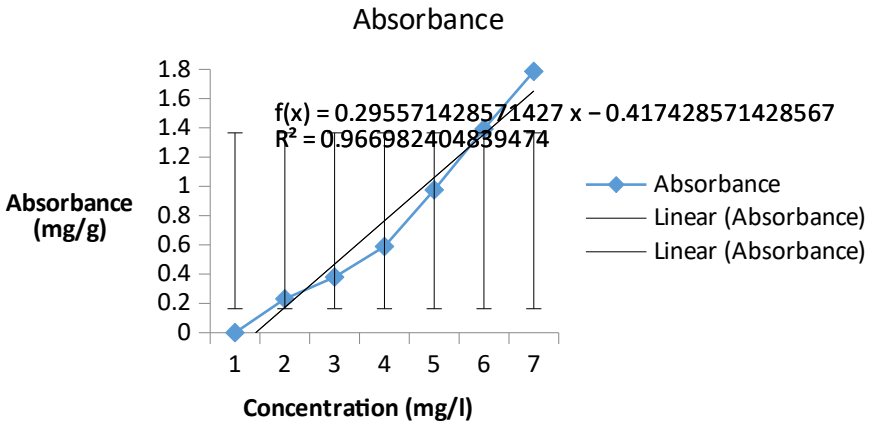

Fig.4.17 at different concentration from 0 to100mg/l phenols' standard calibration curve

Based on the graph, the slope was determined to be 0.017. Therefore, one may determine the ultimate concentration at equilibrium (Ce) at a given time is by multiplying the slope by absorbance. 0.017 x Absorbance is Ce.

4.4.2 Effect of different adsorption parameters

4.4.2.1 PH of solution effect

With 10 mg/L phenol concentration (50mL), 0.4g adsorbent dosage, 2–10 PH range, 120 minutes of contact time ambient temperature had an impact on phenol removal. By addition of 0.1M NaOH or HCl the PH of the solution adjusted, and the result obtained by measuring with a PH meter. From the result it can be seen that adsorption apparatus sensitive to PH. From 2.31 to 2.39 mg/g adsorption capacity increased and then progressively dropped, as PH elevated from 2 to 6 as shown in Fig. 4.15. As Fig. 4.18 illustrates, clearance efficiency increased from 92.55 to 95.63% as pH increased from 2 to 6. Following then, it was also seen that removal efficiency was gradually decreasing. Therefore, it was shown that 6 was the optimal pH for phenol adsorption.

Since phenol has a PKa of 9.89, making it a weak acid, it frequently dissociates at PH>PKa. When PH < PKa is achieved in a phenol solution, the ionic form predominates. This form arises by the ionizing of hydroxyl group causing somewhat negatively charged aromatic ring (equation4.1). Consequently, negatively charged and phenolate ions AC surfaces reject one another electro statically, leading a reduction in adsorption considerably (Nabais et. al., 2019). Adsorption must first defeat the stronger adsorbate-water molecule because these phenolate ions are more soluble in aqueous solution. Kennedy et al. (2020) also shown a similar tendency.

$C_6H_5OH + H_2O \longleftrightarrow C_6H_5O^- + H_3O^+$ (4.1)

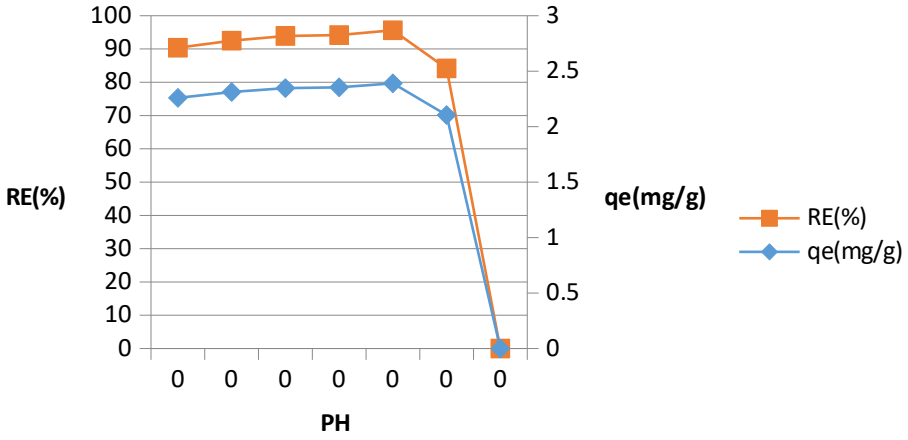

Fig. 4.18: PH effect on removal efficiency and adsorption capacity

4.4.2.2 Adsorbent dose effect

Adsorbent dose is an important factor in testing adsorption, which determines from the given solution adsorbent's capacity for a specific phenol ions initial concentration. One of the main factors affecting the adsorption capacity is quantity of adsorbents in the water. The evaluation of the amount of EL AC adsorbent on efficiency removal is depicted in Fig. 4.19. Using agitation speed=150, contact time=120min, PH=6 and different amounts of EL AC = 0.1 to 0.6g, the batch adsorption investigations were carried out. According to Figure 4.5's data, the adsorption capacity rises from 84.04 to 95.79% at 0.4g of adsorbent before falling at all other dosages. Up to 0.4g, the higher the percentage reduction, the more ion exchangeable sites are available. But after a certain dosage rate of 0.4g, it was shown that the dose rate had no effect on the percentage elimination. The experimental results indisputably demonstrate that as the adsorbent dose greater the elimination efficiency rose and adsorption capacity declined. It explained by as specific quantity of compounds of phenol absorbed depend on the quantity of phenolic ions eliminated to the adsorbent mass, whereas the total amount of phenolic compounds eliminated depend on the number of available binding sites for adsorption process. The increase in adsorbent amount usually fallout in boost in the amount of phenolate ion removed because the adsorbent's increased surface area increases the number of accessible binding sites.

Conversely, the quantity of adsorbent phenol ions per unit weight of the adsorbent decreases as the adsorbent dose increases which could be the result of intricate interactions between several variables. The quantity of phenol dropped slightly as a result of the adsorbent particles in the solution aggregating and overlapping at masses greater than 0.4g, which also resulted in a decrease in the surface area for phenol ion uptake. The results align with the findings of other scholarly investigations (Lee et. al. 2019). This is why the 0.4g mass of adsorbent was utilized for the subsequent testing. A One crucial aspect is that the amount of phenol that can be sorbeted at high adsorbent concentrations is inadequate to entirely cover the available exchangeable sites, which leads to limited adsorption capacity (Nabais et al., 2018).

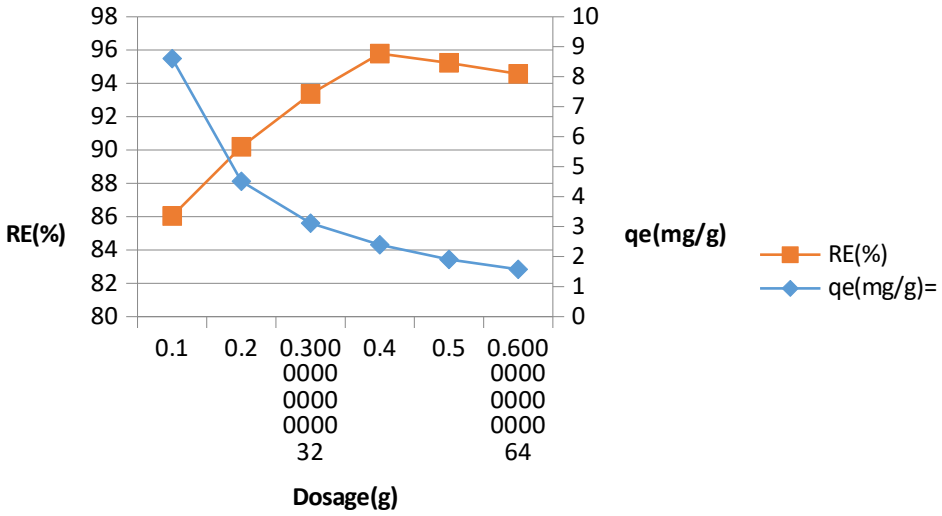

Fig. 4.19 Effect of adsorbent dose on adsorption and removal efficiency

4.4.2.3 Effect of contact time

With a 10 mg/L fixed phenol concentration of (50mL), PH = 6, a 0.4g of adsorbent dose, and a 160 rpm shaker speed, to determine contact duration influence on adsorption of phenol by the produced adsorbent a laboratory test were done. The results are shown in Fig.4.20. The amount of phenol that was adsorbed grew quickly at initially, from 86.04 to 95.79%, before progressively declining until equilibrium was established. This may be a result of saturation of primarily being accessible active sites. Due to the creation of a revolting energy among the adsorbate on the mass phase and on the plane of the adsorbent in addition to the saturation of the active site of the adsorbent, the left over vacant plane sites are consequently hard to take up.

Numerous literary works have noted this trend (Mondal and Kar, 2018). As is evident, phenol's adsorption efficiency grows with increasing duration until it reaches equilibrium within 30min, at which point there is a plateau nature that indicates equilibrium has been reached. The reason might be there were plenty of bulky, accessible adsorption sites, which led to effective electrostatic attraction between the bulk carbon and solute phase (Rambabu 2021).The driving force between phenol and freshly synthesized carbon weakens over time as a result of increased competition amongst phenol molecules for few accessible active sites.

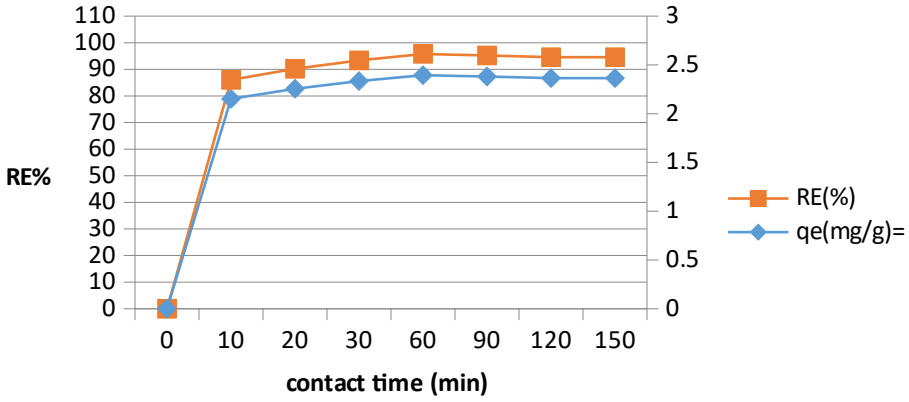

Fig 4.20: Contact time effect on Adsorption capacity and Removal Efficiency

4.4.2.4 Initial concentration effect

Figure 4.21 presented below shows how the capacity of adsorption and elimination capacity influenced by initial phenol concentration. From the figure it can demonstrate the raise in the capacity of adsorption from 2.38 to 8.66mg/g due to a mounting of initial phenol concentration from 10 to 50mg/l. It was discovered that increasing the initial phenol concentration results the capacity of adsorption to rise. It is because any mass transfer barriers that such solutes may have among the solid and liquid phases are effectively pushed aside by the solute's initial concentration in solution. A rise in the concentration serves as a major source of power for the transportation of molecules of phenol to the surface from the bulk solution of the activated Enset leaf. This results in a larger adsorption capacity. This is reliable by way of the conclusion published by Mina et al. (2021).

Furthermore, it was demonstrated that the clearance efficacy dropped by 95.27 to 69.32% since the concentration rise from 10 to 50mg/l. Fixed and saturated adsorption sites may be the cause

of this. The percentage of phenol removed falls as the original phenol concentration rises because additional adsorption cannot be achieved. An analogous tendency was also presented by El-Sayed et. al. (2014).

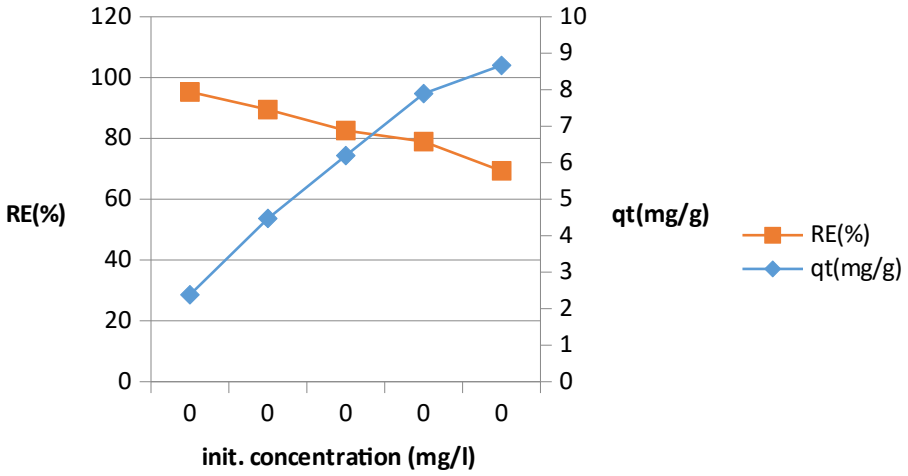

Fig 4.21: Initial concentration effect of on Adsorption capacity and Removal Efficiency

4.4.3 Adsorption isotherms

In order to adequately illustrate the solute adsorptive dynamic parting as of solution with adsorbent, a thorough explanation of the two phase's equilibrium is necessary. According to Allen et al. (2013), while the quantity desorbed and the quantity of solute adsorbed onto the adsorbent equals it is called adsorption equilibrium is achieved. The equilibrium adsorption isotherms were visualized by researchers by plotting q_e, the solid phase concentration of the solute against C_e, the liquid phase concentration. Here, isotherm models of Freundlich, Langmuir, and Temkin were taken to investigate it. In table 4.11, the values of the several constants in the models were calculated and are displayed below.

A. Langmuir Isotherm

By using equation 3.8 from the methodology section the Langmuir's isotherm determined. To examine the Langmuir isotherm model's applicability for phenol elimination by graphing Ce/qe versus Ce the batch adsorption experimental data used. The Langmuir curve of phenol adsorption at PH 6, room temperature, 0.4g of adsorbent dosage, 120minutes of contact duration and for

various beginning phenol concentrations are shown in Fig. 4.7. To compute the Langmuir constants, qm and KL slopes and intercept of the linear plot were used.

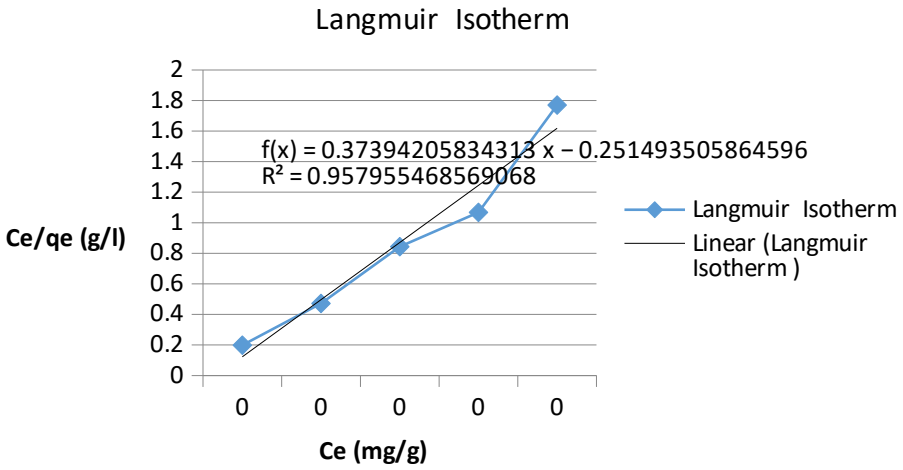

Fig.4.22: Langmuir adsorption isotherm plot

B. Freundlich Isother; By using the logarithmic (equation 3.11) mentioned in the technique section. Figure 4.23 plots the Freundlich isotherm constants as a function of $\log C_e$ and logqe. So, the intercept and slope helped to compute the Freundlich isotherm constants (n and K_F).

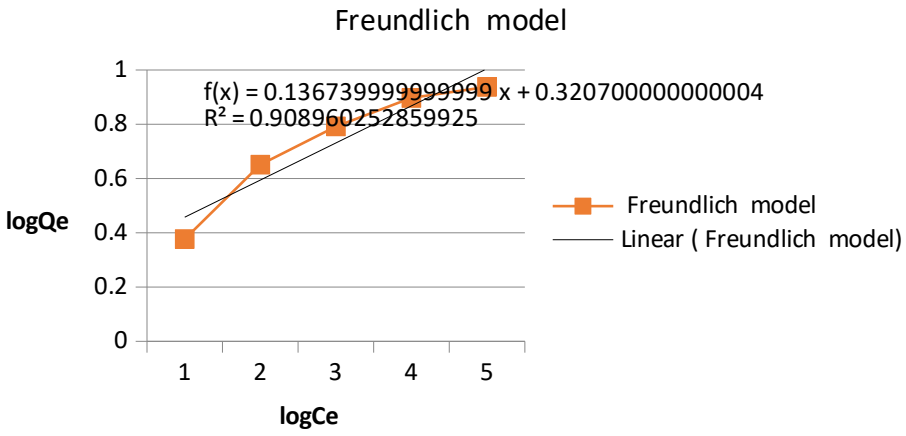

Figure 4.23; Freundlich adsorption isotherm plot

C. Temkin isotherm model

Results of the Temkin isotherm model's linear form were used to the phenol adsorption data, which were acquired from the adsorption of phenol under ideal conditions. The Temkin isotherm parameters were determined by graphing the data in Figure 4.24 of $\ln C_e$ versus q_e. The intercept and slope of the plot of $\ln C_e$vsq_e were used to calculate the Temkin isotherm constants, K_F, and n.

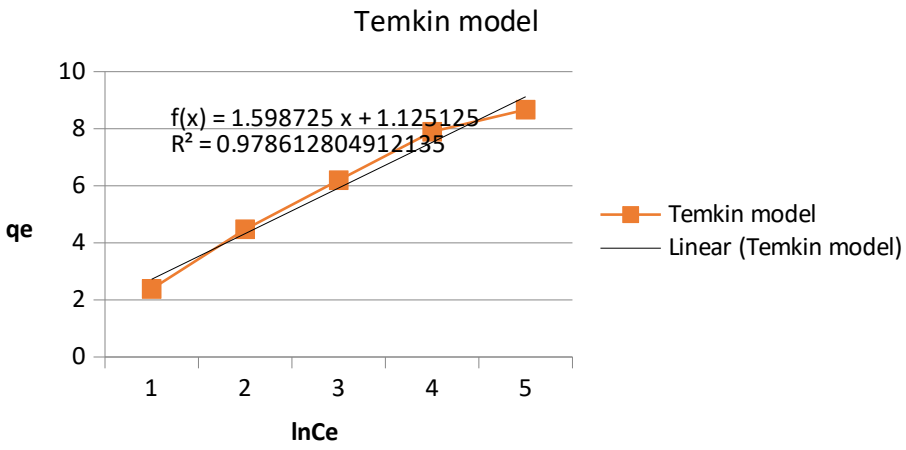

Fig.4.24: Temkin adsorption isotherm plot

From the Langmuir isotherm's parameters computed results, the maximum monolayer adsorption capacity (qm), 5.86mg/g, is greater than the corresponding experimental adsorption capacity (qe,exp). Consequently, EL activated carbon has a high adsorption capacity, as evidenced by the experimentally measured maximum monolayer adsorption capacity (q_m). The process appears to have a high surface energy, which results in a high bonding between the phenol and the EL, based on the comparatively high value of K_L (0.0149L/mg). The low separation factor (R_L) values for a range of starting phenol concentrations were calculated. The results were found to decrease from 0.87 to 0.573 when the concentration increased from 10mg/L to 50mg/L. The finding that $0 < RL < 1$ for the dimensionless component (R_L) implies a successful chemisorption process.

The Freundlich isotherm's parameters were obtained from the logqe vs logCe graph, and the constants KF and n were obtained from the intercept $\log K_F$ and slope 1/n, respectively. It was observed that an adsorption intensity of 7.35 was reached. The table also demonstrates that a chemisorption process, which is incompatible with the previous multilayer physical adsorption

process, is indicated by a value of 1/n (0.141) less than one. It is established that the Enset leaf has a surface heteroginity since n=7.35 satisfies the heterogeneity criteria, 1< n <10 (Boudrahem et al., 2019). Phenol was found to be absorbed onto the adsorbent surface at a rate of 2.089 mg/g, or KF. A parameter in the Temkin isotherm model unambiguously helps for the contact between the adsorbate and adsorbent classes. The process is exothermic, as evidenced by the positive values of the obtained adsorption energy (BT) of 1.598.

The correlation coefficients for the isotherm parameters of each individual model in Table (4.6) were nearly greater and approached unity for the Freundlich isotherm model (R^2=0.909), Langmuir isotherm model (R^2=0.99), and Temkin isotherm model (R^2=0.978). This implies that the Langmuir isotherm model better describes the adsorption of phenol on the EL AC. The strong correlation coefficient (R^2) of 0.99 indicates that phenol is adsorbed onto Enset leaf from an aqueous solution. The suitability of the Langmuir model to the homogenous monolayer on which phenol ions from aqueous solution were adsorbed throughout the adsorption process (Boudrahem et al., 2019)

Table 4.6; Isotherms parameter of phenol removal by Enset leave adsorbent

Isotherm model	Parameters	Values
Langmuir Y=0.102X+0.226	Q_m, Qexp	5.86,2.38mg/g
	K_L(L/mg)	0.0149
	R_L	0.573 to 0.87
	R^2	0.99
Freundlich Y=0.136X+0.32	Kf [(mol/g)(mol/L)n]	2.089
	n	7.35
	R^2	0.909
Temkin Y=1.598X+1.125	β	1.598
	K_T	0.57
	R^2	0.978

4.4.4 Adsorption kinetics

Adsorption kinetic study can help determine the adsorption efficacy. To determine the adsorption mechanism, verify the experimental results and any possible rate-controlling stages, such as

chemical reaction and mass transfer, kinetic models used. The rate, at which a solute is eliminated, controls the amount of time the sorbate remains at the solid-solution interface. So as to ascertain the order of adsorption reactions and rate constants, pseudo-first order and pseudo-second order kinetic models used to the computed kinetic data from the ideal conditions (at solution pH-6, initial phenol concentration of 10mg/L, contact time of 120min, and adsorbent dose of 0.4g/50mL at 150rpm string rate and ambient temperature).

A. Pseudo-First-Order Kinetic Model

The kinetics of a number of distinct adsorption systems have been properly characterized using this model. The values of qe and K_1 are listed in Table 4.7. The observed lower correlation values suggest that the prepared activated carbon phenol adsorption pseudo-first order kinetics is not being followed. The kinetic data and pseudo-first order kinetic model disagrees because boundary layer control over phenol adsorption occurs early on (Boudrahem et al., 2019).

Table 4.7: phenol adsorption experimental results (C_o = 10 mg/L, Volume = 50 ml, optimized pH=6 and optimized dose =0.4g)

t(min)	q_t (mg/l)	q_e (mg/l)	Log ($q_e - q_t$)	t/q_t (min/mg.g-1)
20	2.208	2.3817	**-0.76**	9.057
40	2.364	2.3817	**-1.752**	16.92
60	2.371	2.3817	**-1.971**	32.75
80	2.378	2.3817	**-2.432**	33.64
100	2.38	2.3817	**-2.77**	42.0168
120	2.3815	2.3817	**-3.7**	50.4

B. Pseudo-Second-Order Kinetics Model

Based on the slopes and intercepts of the linear plots made by graphing t/qt vs t, the pseudo-second-order rate constants q_e and K_2 were calculated and are displayed in the table. Figure 4.25 showed the imaginary second order plot of the AC. Very high regression coefficients and excellent conformance with the pseudo-second-order equation were shown by the AC's result. The adsorption of phenol by the generated EL AC followed pseudo second order kinetics, as

indicated by the plots' good fitting and the regression results' R2=0.963 values, which are remarkably close to unity. Furthermore, with correlation values ranging from 0.9 to 1, adsorption experimental data show good correlations with the pseudo-second order rate model.

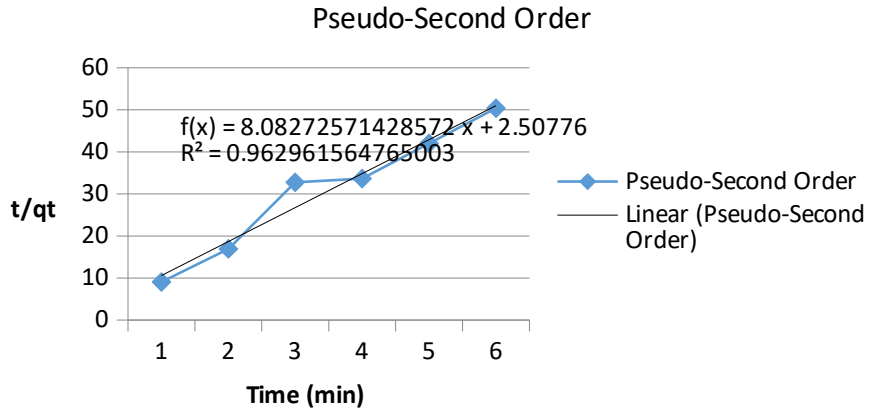

Figure 4.25: Pseudo-Second Order Kinetic Model

From the above, that the kinetic model of pseudo first order should not be used to estimate the adsorption kinetics for the EL AC adsorption. The second order kinetic model, however, has a 0.963 correlation coefficient (R^2). Furthermore, the value of K_2 was found to be greater than the corresponding value of k1, and the experimental (mg/g) values were more closely aligned with the expected qe (mg/g) values derived from pseudo-second-order kinetics. The pseudo-second order kinetic model is therefore determined to be the most appropriate in shape for these adsorption experiments. Consequently, it appeared that a better description of the system under study would be provided by pseudo-second-order kinetics, which was predicated on the idea that the rate-limiting phase may be chemisorptions influencing valence forces through sharing and exchange of electrons. Similar support has been offered by (Tian et al., 2019); this implies chemisorption process significantly manage the rate of.

Table 4.8; pseudo first-order and second order models parameter results

Pseudo first order Kinetic Model y = -0.026X-0.409 R^2 = 0.957	Initial metal conc.(mg/L)	10
	Q_e,cal(mg/g)	2.183
	Q_e,exp(mg/g)	2.3817
	First order rate constant(k_1)	0.058

	Correlation coefficient(R_2)	0.957
Pseudo second order Kinetic Model y = 0.404x + 2.507 R^2 = 0.963	Q_e,cal(mg/g)	2.287
	Q_e,exp(mg/g)	2.1817
	Second order rate constant(k_2) (g/m g)	0.06
	Correlation coefficient(R^2)	0.963
	H	0.36

4.4.5. Statistical analysis

The modeling of phenol adsorption on generated AC5 was done using Design of Experiments (DoE). For modeling the process four-factor, two-level, Full Factorial Design (FFD) was used. Numerous process variables, such as phenol starting concentration, adsorbent dose, PH, and contact time, considered into account in order to create the experimental matrix. The estimated effects of the major elements and how they interact on the answer the optimal conditions for a larger reaction, or a higher percentage of phenol elimination, were ascertained using the Desirability (D) function.

Table 4.9 Factorial design experimental levels and ranges

Factor	Name	Units	Type	Minimum	Maximum	Coded Low	Coded High	Mean	Std. Dev.
A	PH		Numeric	2.00	10.00	-1 ↔ 2.00	+1 ↔ 10.00	6.00	4.13
B	Initial concentration	mg/l	Numeric	10.00	50.00	-1 ↔ 10.00	+1 ↔ 50.00	30.00	20.66
C	Adsorption dos	g/l	Numeric	0.1000	0.5000	-1 ↔ 0.10	+1 ↔ 0.50	0.3000	0.2066
D	contact time	min	Numeric	10.00	150.00	-1 ↔ 10.00	+1 ↔ 150.00	80.00	72.30

4.4.5.1 Modeling of phenol Removal by AC5

A linear regression model for experimental data was built-in by the least squares method. Table 4.10 presented the effects, interactions, model coefficients, , and standard error of the individual components.

Table 4.10 List of model terms estimated regression coefficients and the impacts on the reply for AC5

Source	Sum of Squares	df	Mean Square	F-value	p-value	
Model	3458.93	5	691.79	412.94	< 0.0001	significant
A-PH	143.10	1	143.10	85.42	< 0.0001	
B-Initial concentration	3266.98	1	3266.98	1950.13	< 0.0001	
C-Adsorption dos	0.9950	1	0.9950	0.5939	0.4587	
D-contact time	4.13	1	4.13	2.47	0.1474	
AB	43.73	1	43.73	26.10	0.0005	
Residual	16.75	10	1.68			
Cor Total	3475.69	15				

The statistically significant effects of the model are found using the probability value called the p-value. Factors are considered statistically significant at a 95% confidence level if their p-value is less than 0.05.A, B, and AB are important model terms in this instance. Following the removal of the unnecessary variables, the final model is displayed as follows:

RE% = +79.50 - 2.99 * A+14.29 * B +1.65 * A * B-0.34

The influence of interactions was resoluted using analysis of variance (ANOVA). The significance of the process factor is measured by the sum of its squares (SS), and the linked factor's importance increases with SS value. Table 4.11 presented the results of the ANOVA for the elimination of phenol by AC5.

Table 4.11 ANOVA findings for AC5's phenol removal.

Source	Sum of Squares	df	Mean Square	F-value	p-value	
Model	3458.93	5	691.79	412.94	< 0.0001	significant
A-PH	143.10	1	143.10	85.42	< 0.0001	
B-Initial concentration	3266.98	1	3266.98	1950.13	< 0.0001	
C-Adsorption dos	0.9950	1	0.9950	0.5939	0.4587	
D-contact time	4.13	1	4.13	2.47	0.1474	

AB	43.73	1	43.73	26.10	0.0005	
Residual	16.75	10	1.68			
Cor Total	3475.69	15				

4.4.5.3. Main Effects

Fig. 4.26 shows the main variables and their impact on the result. One of the four main factors that greatly influence the reaction is the amount of phenol present in the solution. The signal for the principal influence shows the way of the consequence. The graph indicates that concentration influences the response positively because of a larger level of divergence from the general mean; by the other side, the percentage of phenol eliminated dropped as PH grew. Adsorbent dosage and contact time are not nearly as important as PH and concentration.

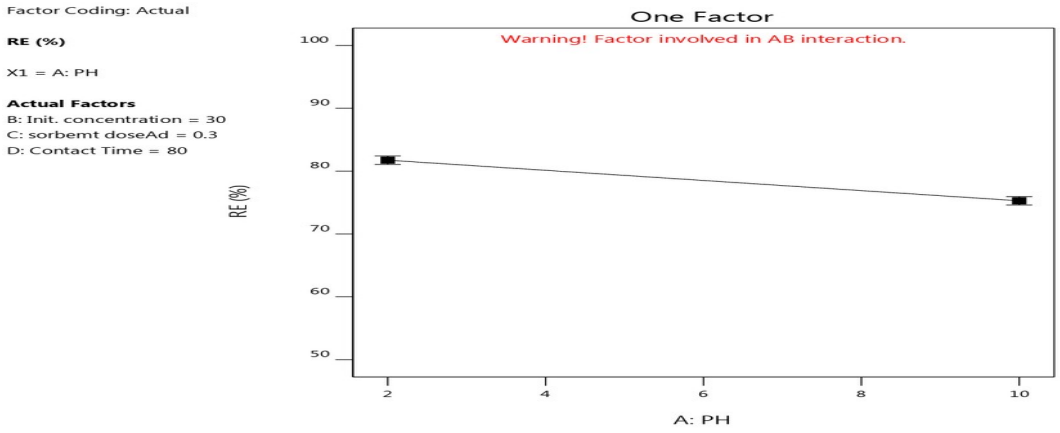

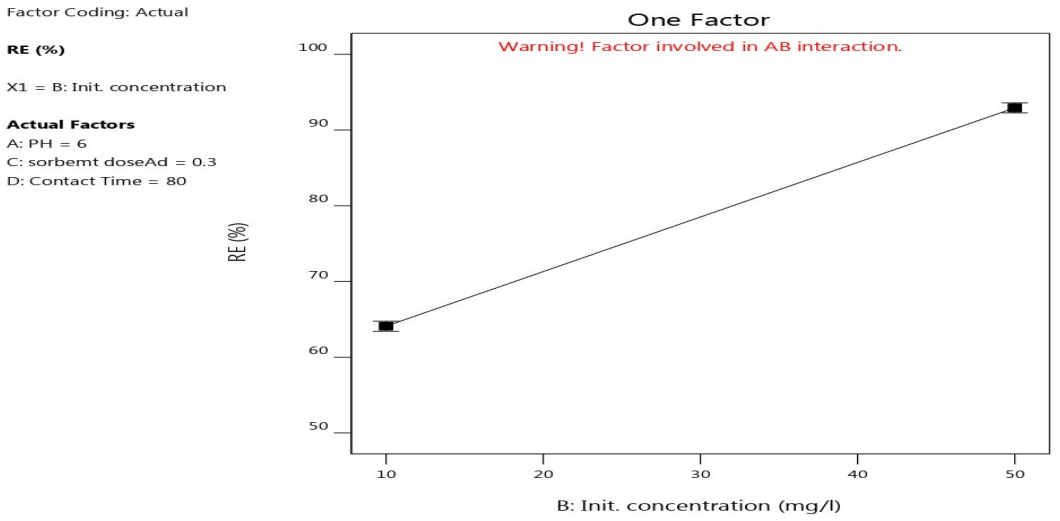

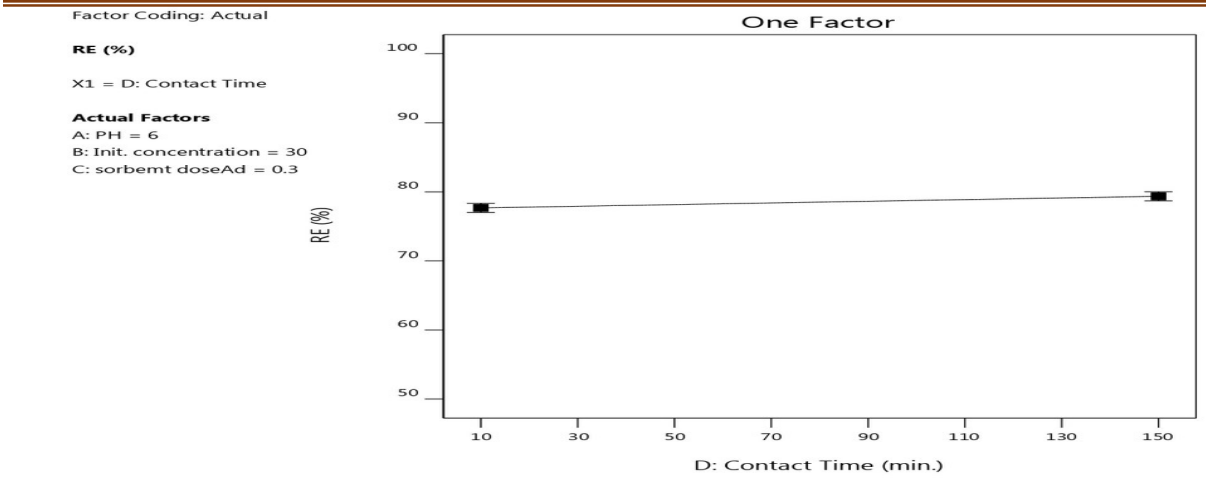

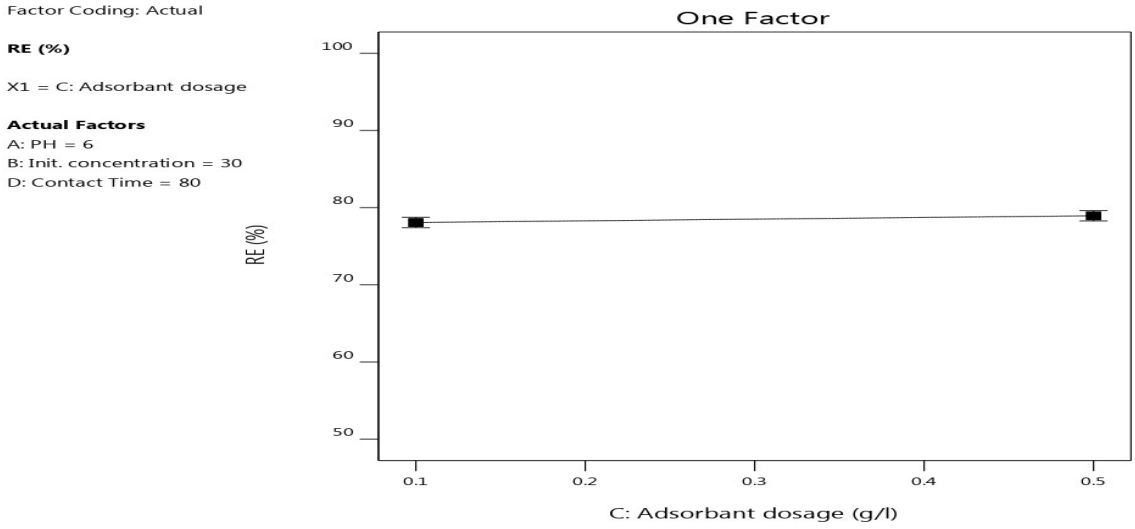

Fig. 4.26: main factors effect on response for AC_5 concentration, PH, contact time and adsorbent dose

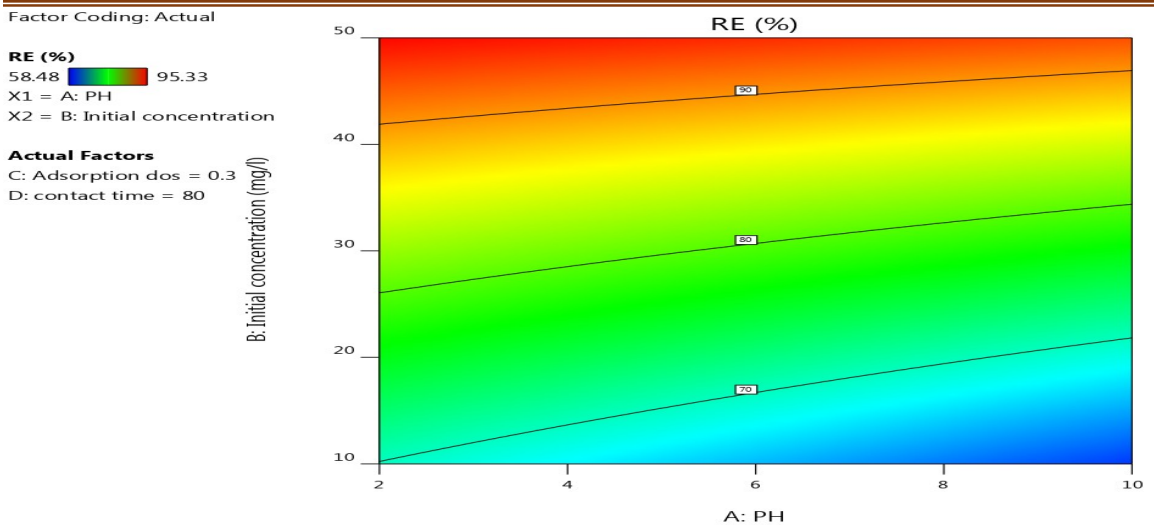

Fig. 4.27 Contour plot for PH * Concentration of interactions for AC5

4.4.5.4 Normal Probability Plot

A straight line connecting the dots indicates if the residuals are normally distributed, as indicated by the normal probability plot. Figure 4.28 shows the normal probability curve of the AC5 residuals for phenol adsorption. The data points' reasonable proximity to a straight line indicates the study population was dispersed frequently.

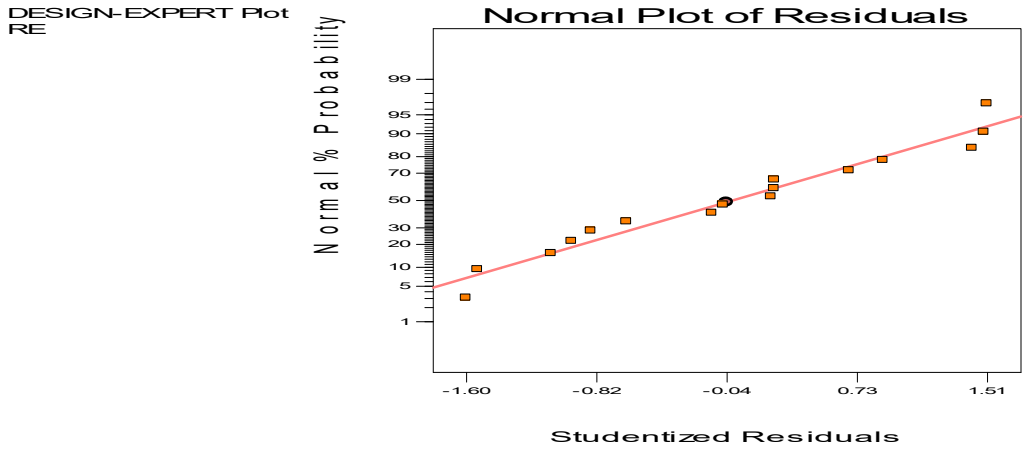

Fig.4.28 Normal probability plot

4.4.5.5. Optimization

In order to remove phenol, the desirability function was utilized to optimize the following factors: initial phenol concentration, PH, contact time, and adsorbent dosage. The aim of optimization is to progress phenol elimination capacity by adjusting the factors to the proper values. In this experiment, contact duration and PH were put within the range under the examination, while the starting concentration was set to be highest amount and the adsorbent dose targeted to the lowest amount within the range.

Figure 4.29 displays the contour and 3D surface plot of AC5's phenol elimination.

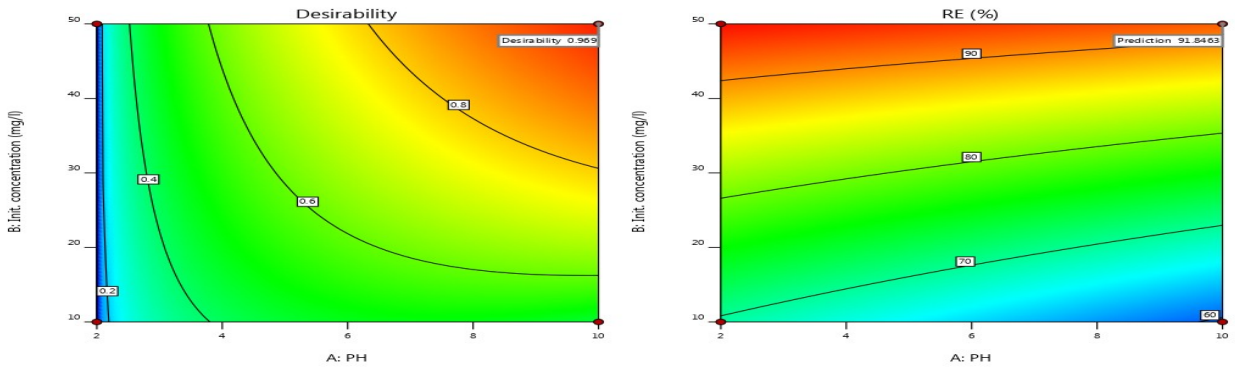

Fig. 4.29 Contour plot desirability function

4.4.5.6. Validation Experiments

An experiment was carried out in settings that the established model predicted in order to validate the optimization outcomes. The model estimated that 90.42% of the phenol would be removed at pH = 6, initial concentration of 30mg/L, 80min of contact time and 0.3g/L adsorbent dosage. The results of the optimization were validated by the experimental value obtained under these circumstances, which was 88.68% and closely matched the model's outcome.

Table 4.12 the predicted optimization values of process control parameters

Factor	Name	Units	Type	Minimum	Maximum	Coded Low	Coded High	Mean	Std. Dev.
A	PH		Numeri	2.00	10.00	-1 ↔	+1 ↔	6.00	4.13

			c			2.00	10.00		
B	Initial concentration	mg/l	Numeric	10.00	50.00	-1 ↔ 10.00	+1 ↔ 50.00	30.00	20.66
C	Adsorption dos	g/l	Numeric	0.1000	0.5000	-1 ↔ 0.10	+1 ↔ 0.50	0.3000	0.2066
D	contact time	min	Numeric	10.00	150.00	-1 ↔ 10.00	+1 ↔ 150.00	80.00	72.30

4.5 Comparison with other ACs

Table 4.13 comparison of EL AC with other ACs

Precursor	**Modification process**	**Surface Area (m2/g)**	**Reference**
Enset leaf	H_3PO_4 activation	268 - 1023	Present work
Rice Husk	H_3PO_4 activation	634 - 1820	Li et al. (2011b)
Cotton stalk	H_3PO_4 activation	330 - 1720	Nahil& Williams (2012)
Date palm pit	H_3PO_4 activation	725	Reddy et. al. (2012)

5. CONCLUSION AND RECOMMENDATION

5.1 Conclusion

This research is important because it investigates further methods for removing phenol from water. Consequently, the study's research indicates that the EL is a good precursor for activating carbon due to its high carbon concentration. It is preferred in this study to use a chemical activation procedure with typical chemical activators such phosphoric acid. Broad study has been prepared too on the effect of various preparation parameters on surface area and formation of pore of the AC made from EL. The results clearly show that smaller particle sizes are preferred for usage as chemically AC because of the greater surface area exposed during impregnation and activation. Additionally, a relatively modest impregnation ratio is necessary to inhibit the creation of healthy pores. In addition, if EL is used as a precursor, the carbonization temperature should not be higher than 500°C since this will cause the activated carbon's porous formation to break down and lessen the amount of surface area that is available for the adsorption process. Sample AC5 (IR=1, carbonization temperature=500°C, activation temperature=60min) performed better than the other samples due to its remarkable N_2 adsorption-desorption isotherm, and BET surface area which suggests micro- and meso- porosity. Ultimately, it was shown that employing activated carbon derived from EL, phenol could be eliminated via adsorption.

5.2 Recommendation

By thoroughly examining the adsorption and desorption processes while employing AC prepared from EL as an adsorbent, the research can be moved forward to the next level of investigation. When talking about adsorption, a number of factors can be considered, such as the temperature and the rate at which the adsorption process is mixed. For this study, a significant number of samples from the project with the highest BET (sample AC5) will be generated. This aids in determining the ideal circumstances in which the greenhouse gas will be absorbed on the reactive sites of the AC made from EL.

Furthermore, it might be worthwhile to look into the feasibility of employing different biomass or agricultural wastes as a sample for the creation of AC. The removal capacity of AC produced from various samples will vary depending on the process parameters. More evidences can be

gained by comparing studies employing various source documents so as to discover an improved bio-sorbent to get rid of wastes. Since a result, research into producing adsorbent from farming desecrate could be a immense subject to concentrate on, since it provides a more cost-effective and environmentally friendly way to keep the environment free of pollutants.

REFERENCES

Abbas, S.T. (2013). Modeling and optimization of adsorption of heavy metal ions onto local activated carbon. Aquatic Science and Technology, 1(2), 108-134

Abdelkreem, M. (2013). Adsorption of phenol from industrial wastewater using olive mill waste. APCBEE Procedia, 5, 349 – 357

Achmad, A., Jain, K., Tong, K.S., Rozaini, C.A. and Tan, L.S. (2012). Equilibrium, kinetic and thermodynamic studies on the adsorption of direct dye onto a novel green adsorbent developed from Uncaria Gambir extract. Journal of Physical Science, 23(1), 1–13

Ahmaruzzaman, Md. Adsorption of phenolic compounds on low-cost adsorbents: A review. Advances in Colloid and Interface Science, 143 (1-2), 2008, 48-67.

Agarry, S.E. and Aremu, M.O. (2012a). Batch equilibrium and kinetic studies of simultaneous adsorption and biodegradation of phenol by pineapple peels immobilized Pseudomonas Aeruginosa NCIB 950. British Biotechnology Journal, 2(1), 26-48

Ahmad, A.A. and Hameed, B.H. (2010). Effect of preparation conditions of activated carbon from bamboo waste for real textile wastewater. Journal of Hazardous Materials, 173, 487–493

Amin, N.K (2008). Removal of reactive dye from aqueous solutions by adsorption onto activated carbons prepared from sugarcane bagasse pith. Desalination, 223, 152– 161

Arami-Niya, A., Daud, W.M.A.W., Mjalli, F.S. Comparative study of the textural characteristics of oil palm shell activated carbon produced by chemical and physical activation for methane adsorption. Chemical Engineering Research and Design, 89 (6), 2019, 657-664.

Bada, S.O. (2007). Adsorption of Phenols onto Fly Ash. M. Eng Thesis, University of the Witwatersrand, South Africa. Bagheri, N. and Abedi, J. (2009). Preparation of high surface area activated carbon from corn by chemical activation using potassium hydroxide. Chemical Engineering Research and Design, 87, 1059–1064

Bansal, M., Garg, U., Singh, D. and Garg, V.K. (2009). Removal of Cr (VI) from aqueous solutions using pre-consumer processing agricultural waste: A case study of rice husk. Journal of Hazardous Materials, 162, 312–320

Baseri, R.J., Palanisamy, P.N. and Sivakumar, P. (2012). Preparation and Characterization of Activated Carbon from Thevetia Peruviana for the Removal of Dyes from Textile Wastewater, Advances in Applied Science Research, 3(1), 377-383

Basonde, R.R (2002). Treatment of Organic and Inorganic Pollutants in Municipal Wastewater by Agricultural By-Product Based Granular Activated Carbons. M. Tech Thesis, Louisiana State University, Louisiana, USA.

Boehm, H.P. Some aspects of the surface chemistry of carbon blacks and other carbons. Carbon, 32 (5), 2017, 759-769.

Calero, M., Ronda, A., Martın-Lara, M.A., Perez, A. and Blazquez, G. (2013). Chemical activation of olive tree pruning to remove lead (II) in batch system: Factorial design for process optimization. Biomass and Bioenergy, 58, 322-332

Ceyhan, A. A., Sahin, O., Saka, C. and Yalcın, A. (2013). A novel thermal process for activated carbon production from thevetch biomass with air at low temperature by two-stage procedure. Journal of Analytical and Applied Pyrolysis, 104, 170–175

Chand, R., Watari, T., Inoue, K., Kawakita, H., Luitel, H.N., Parajuli, D., Torikai, T. and Yada, M. (2009). Selective adsorption of precious metals from hydrochloric acid solutions using porous carbon prepared from barley straw and rice husk. Minerals Engineering, 22, 1277–1282

Chen, N., Zhang, Z., Feng, C., Li, M., Suiguira, N. and Chen, R. (2011a). Investigation on the batch and fixe-bed column performance of floride adsorption by kanuma mud. Desalination, 268, 76-82

Demiral, H., Demiral, I., Tumsek, F., Karabacakoglu, B. Pore structure of activated carbon prepared from hazelnut bagasse by chemical activation. Surface and Interface Analysis, 40, 2008, 616-619.

Deng, H., Li, G., Yang, H., Tang, J. and Jiangyun, T. (2010). Preparation of activated carbons from cotton stalk by microwave assisted KOH and K2CO3 activation. Chemical Engineering Journal, 163, 373–381

Djebbar, M., Djafri1, F., Bouchekara, M. and Djafri, A. (2012). Adsorption of phenol on natural clay. African Journal of Pure and Applied Chemistry, 6(2), 15-25

El-Hendawy, A.N.A. Influence of HNO3 oxidation on the structure and adsorptive properties of corncob-based activated carbon. Carbon, 41, 713-722.

Elibol, M., Response surface methodological approach for inclusion of perfluorocarbon in actinorhodin fermentation medium. Process Biochemistry, 38, 2002, 667-673.

Emmet, P.H., Brunauer, S. The use of low temperature van der waals adsorption isotherms in determing the surface area of iron synthetic ammonia catalysts. Journal of American Chemical Society, 1937, 59 (8), 1553-1564.

Girish, C.R. and Ramachandra, M.V. (2012). Adsorption of phenol from wastewater using locally available adsorbents. Journal of Environmental Research and Development, 6(3a), 763-772

Guo, Y., Rockstraw, D.A., Activated carbons prepared from rice hull by one-step phosphoric acid activation. Microporous and Mesoporous Materials, 100, 2007, 12-19.

Hai, F.I., Yamamoto, K., Nakajima, F., Fukushi, K. Bioaugmented membrane bioreactor (MBR) with a GAC – packed zone for high rate textile wastewater treatment. Water Research, 45 (6), 2011, 2199-2206. Haimour, N.M., Emeish, S., Utilization of date stones for production of activated carbon using phosphoric acid. Waste Management, 26 (6), 2006, 651-660.

Hamadi, N.K., Chen,X.D., Farid, M.M., Lu, M.G.Q. Adsorption kinetics for the removal of chromium(VI) from aqueous solution by adsorbents derived from used tyres and sawdust. Chemical Engineering Journal, 84, 2001, 95-105.

Ho, Y.S., McKay, G. Biosorption of dye from aqueous solution by peat. Chemical Engineering Journal, 70, 1998, 115-124

Jagtoyen M, Derbyshire F. Activated carbons from yellow poplar and white oak by H3PO4 activation. Carbon, 36, 1998, 1085-1097.

Kawano, T., Kubota, M., Onyango, M.S., Watanabe, F., Matsuda, H. Preparation of activated carbon from petroleum coke by KOH chemical activation for adsorption heat pump. Applied Thermal Engineering, 28, 2008, 865-871.

Lai, K.C., Lo, I.M. Removal of chromium (VI) by acid-washed zero-valent iron under various ground water geochemistry conditions. Environmental Science & Technology, 42, 2008, 1238-1244.

Langmuir, I. The adsorption of gases on plane surfaces of glass, mica, and platinum. Journal of American Chemical Society, 40 (9), 1918, 1361-1403.

Lee, Y.W., Choi, D.K., Park, J.W. Performance of fixed-bed KOH impregnated activated carbon adsorber for NO and NO2 removal in the presence of oxygen. Carbon, 40 (9), 2002, 1409- 1417

Liu, Z.S. Adsorption of SO2 and NO from incineration flue gas onto activated carbon fibers. Waste Management, 28 (11), 2019, 2329-2335.

Madhava Rao, M., Kumar Reddy, D.H.K., Venkateswarlu, P., Seshaiah, K. Removal of mercury from aqueous solutions using activated carbon prepared from agricultural by-product/waste. Journal of Environmental Management, 90 (1), 2019, 634-643.

Mishra, S. Report on Design of a cheap water filter for chromium contaminated water. Water initiative technology, DST, India

Mohammadi, S.Z., Karimi, M.A., Afzali, D., Mansouri, F. Removal of Pb(II) from aqueous solutions using activated carbon from sea-buckthorn stones by chemical activation. Desalination, 262 (1-3), 2010, 86-93.

Zhang, J., Fu, H., Lu, X., Tang, J., Xu, X. Removal of Cu(II) from aqueous solution using the rice husk carbons prepared by the physical activation process. Biomass and Bioenergy, 35, 2011, 464-472